

STABILITY OF SODIUM SULFATE DICARBONATE
(~2Na₂CO₃•Na₂SO₄) CRYSTALS

A Thesis
Presented to
The Academic Faculty

by

Cosmas Bayuadri

In Partial Fulfillment
of the Requirements for the Degree
Master of Science in Paper Science and Engineering in the
School of Chemical and Biomolecular Engineering

Georgia Institute of Technology
August 2006

Copyright © Cosmas Bayuadri 2006

STABILITY OF SODIUM SULFATE DICARBONATE

(~2Na₂CO₃•Na₂SO₄) CRYSTALS

Approved by:

Dr. Ronald W. Rousseau, Advisor
School of Chemical and Biomolecular Engineering
Georgia Institute of Technology

Dr. W. James Frederick Jr.
Institute of Paper Science and Technology at
Georgia Institute of Technology

Dr. Christopher L. Verrill
Institute of Paper Science and Technology at
Georgia Institute of Technology

Date Approved: May 10, 2006

ACKNOWLEDGEMENTS

First of all, I would like to express my deepest sense of gratitude to my supervisor Professor Ronald W. Rousseau for his patient guidance, encouragement and excellent advice throughout this study. My sincere thank to Dr. Christopher L. Verrill for his continuous guidance, assistance, and advice encouragement.

I wish to thank the remaining member of my thesis committee Dr. W. James Frederick, Jr., for his valuable input to this research.

I would like to express my gratitude to Institute of Paper Science and Technology at Georgia Tech and member companies for my study and research support.

I am thankful to Steve Lien, Alan Ball, Jeff Champine, and Dr. Nikolai DeMartini from Institute of Paper Science and Technology at Georgia Tech for their generous assistance during this time. The author also thanks Dr. Xin-Sheng Chai from Institute of Paper Science and Technology at Georgia Tech for insightful discussions and performing the thermal analysis.

TABLE OF CONTENTS

ACKNOWLEDGEMENTS	ii
LIST OF TABLES	v
LIST OF FIGURES	vi
NOMENCLATURE	x
SUMMARY	xi
CHAPTER 1 INTRODUCTION	1
1.1 Origin of Sodium Sulfate Dicarboxate	1
1.2 Hypotheses and Problems	2
1.3 Objectives	3
CHAPTER 2 BACKGROUND	4
2.1 Crystallization	4
2.1.1 Supersaturation	7
2.1.2 Nucleation	10
2.1.3 Metastable Zone	10
2.1.4 Crystal Growth	11
2.1.5 Agglomeration	12
2.1.6 Crystal Aging	12
2.2 Previous Research	13
2.3 Double Salt Crystals Stability	15
2.3.1 Stability Identification	15
CHAPTER 3 EXPERIMENTAL APPARATUS AND PROCEDURES	18
3.1 Equipments and Procedures	18
3.1.1 Equipments	18
3.1.2 Solution Preparation	21
3.1.3 Evaporative Crystallization	21

3.2 Analysis Methods.....	23
3.2.1 Particle Vision and Measurement (PVM) and Focused Beam Reflectance Measurement.....	23
3.2.2 Powder X-Ray Diffraction (XRD).....	24
3.2.3 Differential Scanning Calorimetry (DSC)	24
3.2.4 Thermogravimetric Analysis (TGA).....	25
3.2.5 Polarized Light Microscopy (PLM).....	26
3.2.6 Thermal Exposure.....	27
CHAPTER 4 RESULTS AND DISCUSSION.....	28
4.1 Development of Crystal Isolation Procedure.....	28
4.2 Stability of Sodium Sulfate Dicarboxate and Thermonatrite Crystals Mixture	36
4.3 Thermal Stability of Burkeite Crystals	44
4.4 Stability of Sodium Sulfate Dicarboxate Crystals	47
4.5 Stability of Crystal Samples on Storage	57
CHAPTER 5 CONCLUSIONS AND RECOMMENDATIONS	61
5.1 Conclusions.....	61
5.2 Recommendations.....	62
5.2.1 Molecular level stability investigation.....	62
5.2.2. Properties of different sodium sulfate dicarboxate crystal habits...	63
APPENDIX A: POLARIZED LIGHT MICROGRAPHS OF SODIUM SALT	64
APPENDIX B: POWDER X-RAY DIFFRACTIONS OF SODIUM SALTS.....	69
REFERENCES	79

LIST OF TABLES

Table 2.1.1 Seven unique crystal systems from Wikipedia.org (Crystal Structure, 2006).	5
Table 4.1.1 Primary nucleation delay when the evaporation of solution with 6:1 molar ratio of Na_2CO_3 to Na_2SO_4 was stopped earlier.	30
Table 4.1.2 Phase identifications from the XRD results on Figure 4.1.1	32

LIST OF FIGURES

Figure 2.1.1 Zone divisions on solution system with inverse solubility.....	6
Figure 2.1.2 Solubilities of sodium salts and burkeite in water. Data adapted from Shi (2002), based on his work and various sources including Seidell and Linke (1965), Green & Frattali (1946), Frederick & DeMartini (1999).	7
Figure 2.3.1 DSC scan of anhydrous Na_2CO_3 shows polymorph transition at 350°C	17
Figure 2.3.2 DSC scan of anhydrous Na_2SO_4 shows polymorph transition at 238 and 248°C	17
Figure 3.1.1 Schematic diagram of 1 liter bench-scale batch crystallizer	18
Figure 3.1.2 Schematic diagram and photograph of 3 liter bench-scale batch crystallizer	19
Figure 3.1.3 Porous stainless steel 2 micron filter cartridge used in crystal isolating procedures.	20
Figure 3.2.1 Simple schematic representation of the tip of the Lasentec® FBRM probe	23
Figure 3.2.2 DSC Pyris 1 from PerkinElmer	25
Figure 3.2.3 Polarized light micrograph of a single $\text{Na}_2\text{CO}_3 \cdot \text{H}_2\text{O}$ (Thermonatrite) crystal shows maximum birefringence at 45° rotation.....	27
Figure 4.1.1 XRD analysis result of crystals from the evaporation of the solution containing various molar ratio of Na_2CO_3 to Na_2SO_4 at 100°C . (See Appendix B, Figure B3).....	31
Figure 4.1.2 DSC Scan of crystals from the evaporation of the solution containing various molar ratio of Na_2CO_3 to Na_2SO_4 at 100°C	32
Figure 4.1.3a PVM image of crystals from early nucleation from evaporation of aqueous solution of Na_2CO_3 and Na_2SO_4 with 6:1 molar ratio at 115°C without EDTA taken at point A in Figure 4.1.3b at 2:17 PM.	34
Figure 4.1.3b FBRM data for evaporation of aqueous solution of Na_2CO_3 and Na_2SO_4 with 6:1 molar ratio at 115°C without EDTA.	34
Figure 4.1.3c PVM image of crystals from early nucleation from evaporation of aqueous solution of Na_2CO_3 and Na_2SO_4 with 6:1 molar ratio at 115°C without EDTA taken at point B in Figure 4.1.3b at 2:19 PM. Some hexagonal structures appeared which later on identified as sodium sulfate dicarbonate.	35
Figure 4.1.4a PVM image of crystals from early nucleation from evaporation of aqueous solution of Na_2CO_3 and Na_2SO_4 with 6:1 molar ratio at 115°C with EDTA taken at point A in Figure 4.1.4b at 10:34 AM.	35

Figure 4.1.4b FBRM data for evaporation of aqueous solution of Na_2CO_3 and Na_2SO_4 with 6:1 molar ratio at 115°C with EDTA.	36
Figure 4.2.1 Experimental diagram that resulted in a mixture of sodium sulfate dicarbonate and thermonatrite crystals.....	37
Figure 4.2.2 FBRM data for 6 hours crystal aging experiment with a solution of 6:1 molar ratio of Na_2CO_3 to Na_2SO_4 without EDTA.....	38
Figure 4.2.3 XRD analysis of a mixture of sodium sulfate dicarbonate and thermonatrite crystals obtained from evaporation of an aqueous solution of Na_2CO_3 and Na_2SO_4 (6:1 mole ratio, without EDTA) after aging samples 0, 3 and 6 hours rinsed with ethanol. (See Appendix B, Figure B5).	39
Figure 4.2.4 Chemical composition analysis of aged crystal mixtures washed in ethanol shows an increase in carbonate to sulfate ratio.	40
Figure 4.2.5 DSC scan of a crystal mixture sample harvested after 6 h aging showing an apparent overlap of two individual peaks in the range 78-140 °C due to evaporation of ethanol and dehydration of $\text{Na}_2\text{CO}_3 \cdot \text{H}_2\text{O}$	41
Figure 4.2.6 TGA analysis of the crystal mixture analyzed in Figure 4.2.4.....	42
Figure 4.2.7 XRD analysis of crystal mixture of sodium sulfate dicarbonate and thermonatrite harvested after 6 h aging before and after exposure to 200 °C. (See Appendix B, Figure B6).....	43
Figure 4.2.8. Photomicrographs of the sodium sulfate dicarbonate-thermonatrite mixture before (a) and after (b) exposure to 200 °C.....	43
Figure 4.3.1 Experimental diagram to investigate stability of burkeite crystals.	45
Figure 4.3.2 XRD analysis of burkeite crystals from evaporation of 1:2 molar ratio of aqueous solution of Na_2CO_3 and Na_2SO_4 before and after heat exposure to 200°C shows relatively no change in structure.	45
Figure 4.3.3 Two sequential DSC scans of a single sample of burkeite crystals.	46
Figure 4.4.1 Experimental diagram to investigate stability of sodium sulfate dicarbonate crystals.....	48
Figure 4.4.2 XRD analysis of sodium sulfate dicarbonate crystals obtained from evaporation of an aqueous solution of Na_2CO_3 and Na_2SO_4 at 6:1 molar ratio with EDTA; sampled after aging 0 and 24 hours.	48
Figure 4.4.3 PLM observation on sodium sulfate dicarbonate from evaporation of salt solution with EDTA.	49
Figure 4.4.4 FBRM data during crystal aging experiment without EDTA shows chord counts, temperature and pressure measurements up to 34 hours.	50
Figure 4.4.5 XRD analysis of sodium sulfate dicarbonate crystals obtained from evaporation of an aqueous solution of Na_2CO_3 and Na_2SO_4 (6:1 mole ratio, without EDTA) after aging samples 12, 18 and 34 hours (ethylene glycol + ethanol rinsed).	51

Figure 4.4.6 Transformation of crystal composition when aged in mother liquor having a 6:1 mole ratio of sodium carbonate to sodium sulfate at 115 °C.	52
Figure 4.4.7 Photomicrographs of the sodium sulfate dicarbonate from evaporation of solution without EDTA showing coexistence of two different crystal habits, agglomerated rods and hexagonal shapes.	53
Figure 4.4.8 3-D schematic representations of sodium sulfate dicarbonate shapes based on PLM images on Appendix A. Drawn using George Favreau's FACES v.3.7 software.	54
Figure 4.4.9 DSC scan of sodium sulfate dicarbonate from evaporation of the salt solution with EDTA shows features of residual ethanol and ethylene glycol (crystal washing solvent) release.	55
Figure 4.4.10 XRD analysis of sodium sulfate dicarbonate obtained from evaporation of an aqueous solution of Na_2CO_3 and Na_2SO_4 (mole ratio 6:1) with EDTA before and after exposure to 200 °C.	56
Figure 4.4.11 Photomicrographs of sodium sulfate dicarbonate crystals before (left) and after (right) heating to 200°C.	57
Figure 4.5.1 Photomicrograph showing possible trona formation in between sodium sulfate dicarbonate crystals due to prolonged exposure to ambient air.	58
Figure 4.5.2 XRD results on sodium sulfate dicarbonate crystals stored for extended period of time in ambient air.	59
Figure 4.5.3 XRD results on sodium sulfate dicarbonate crystals stored for extended period of time under vacuum.	59
Figure A.1 Anhydrous Sodium Sulfate.....	64
Figure A.2 Anhydrous Sodium Carbonate.....	64
Figure A.3 Sodium Carbonate Monohydrate (transparent crystals) with Sodium Sulfate Dicarbonate Agglomerates (dark agglomerates).....	65
Figure A.4 Hexagonal Sodium Sulfate Dicarbonate aged for 12 hours without immersion medium shows hexagonal structure agglomerated like a flower petal.	65
Figure A.5 Sodium Sulfate Dicarbonate aged for 12 hours immersed in Ethylene Glycol shows optical birefringence at different rotation angles.	66
Figure A.6 Sodium Sulfate Dicarbonate aged for 12 hours (left) and 18 hours (right) immersed in Ethylene Glycol shows the hexagonal structure can grow from agglomerated core or a single rod crystal.	66
Figure A.7 Agglomerated rod-like crystals identified as Sodium Sulfate Dicarbonate (aged for 18 hours) immersed in Ethylene Glycol.....	67
Figure A.8 Hexagonal Sodium Sulfate Dicarbonate (aged for 18 hours) growing outward from a core single or agglomerated rod-like crystal.	67
Figure A.9 Hexagonal Sodium Sulfate Dicarbonate (aged for 12 hours) showing colorful light refraction indicates crystal plane of {3, 1, 4}.	68

Figure B.1 Powder X-ray Diffraction of reagent anhydrous Sodium Carbonate crystals used in this work	69
Figure B.2 Powder X-ray Diffraction of anhydrous Sodium Sulfate crystals used in this work.....	70
Figure B.3 Powder X-ray Diffraction of crystals from evaporation of the solution containing various molar ratio of Na_2CO_3 to Na_2SO_4 at 100°C	71
Figure B.4 Powder X-ray Diffraction of crystals from evaporation of aqueous solution of Na_2CO_3 to Na_2SO_4 at 1:1 mole ratio (100°C) shows a mixture of burkeite and thermonatrite.	72
Figure B.5 Powder X-ray Diffraction of a mixture of sodium sulfate dicarbonate and thermonatrite crystals obtained from evaporation of an aqueous solution of Na_2CO_3 and Na_2SO_4 (6:1 mole ratio, without EDTA) after aging samples 0 (304A), 3 (304B) and 6 (304C) hours rinsed with ethanol.	73
Figure B.6 Powder X-ray Diffraction of crystal mixture of sodium sulfate dicarbonate and thermonatrite harvested after 6 hours aging before and after exposure to 200°C	74
Figure B.7 Powder X-ray Diffraction of a mixture from anhydrous Na_2CO_3 and anhydrous Na_2SO_4 at 1:2 mole ratio shows integration of peaks from individual characteristic patterns.....	75
Figure B.8 Powder X-ray Diffraction of crystals from evaporation of an aqueous solution of Na_2CO_3 and Na_2SO_4 at 6:1 mole ratio (100°C) shows large thermonatrite content.	76
Figure B.9 Powder X-ray Diffraction of sodium sulfate dicarbonate crystals from evaporation of an aqueous solution of Na_2CO_3 and Na_2SO_4 at 6:1 mole ratio (115°C) with EDTA; sampled after aging 0 (CS61E3) and 24 hours (CS61E5).....	77
Figure B.10 Powder X-ray Diffraction of sodium sulfate dicarbonate crystals from evaporation of an aqueous solution of Na_2CO_3 and Na_2SO_4 at 6:1 mole ratio (115°C) without EDTA; sampled after aging 12 (COSMASH3), 18 (COSMASH5) and 34 hours (COSMASH7).	78

NOMENCLATURE

c_i	solute species i concentration
c_i^*	solute species i concentration at equilibrium
D	Diameter, m
ΔG_i	overall free energy change to form a cluster of i molecules, J mole ⁻¹
m	mass, kg
N	impeller rotation per second
N_{Re}	Reynolds number
R	gas constant, J mol ⁻¹ K ⁻¹
S	supersaturation ratio
T	Temperature, K, °C
t	time, hour, second
x	mole fraction

Greek Symbols

α	activity
γ	activity coefficient
σ	relative supersaturation
μ	chemical potential, J mole ⁻¹
μ°	chemical potential at standard state, J mole ⁻¹
μ	viscosity Pa.s
ρ	solution density, kg m ⁻³

SUMMARY

Research on salts species formed by evaporation of aqueous solution of Na_2CO_3 and Na_2SO_4 began in the early 1930s. The thermodynamic, crystallographic and many other physical and chemical properties of most of the species formed from this solution has been known for decades. However, there was no complete information or reliable data to confirm the existence of a unique double salt that is rich in sodium carbonate, up until five years ago when a Bing Shi identified the double salt ($\sim 2\text{Na}_2\text{CO}_3 \cdot \text{Na}_2\text{SO}_4$) from the ternary system $\text{Na}_2\text{CO}_3 - \text{Na}_2\text{SO}_4 - \text{H}_2\text{O}$ (Shi, 2002 *Crystallization*).

Crystallization of this double salt so called sodium sulfate dicarbonate ($\sim 2\text{Na}_2\text{CO}_3 \cdot \text{Na}_2\text{SO}_4$) is known to be a primary contributor to fouling heat-transfer equipment in spent-liquor concentrators used in the pulp and paper industry. Therefore, understanding the conditions leading to formation of this double salt is crucial to the elimination or reduction of an industrial scaling problem.

In this work, double salts were generated in a batch crystallizer at close to industrial process conditions. X-ray diffraction, calorimetry, and microscopic observation were used to investigate the stability of the salts to in-process aging, isolation and storage, and exposure to high temperature.

The results show that care must be taken in sampling during evaporative crystallization. Two apparent crystal habits were detected in the formation of sodium sulfate dicarbonate; the favored habit may be determined by calcium ion impurities in the system.

The results also verify that sodium sulfate dicarbonate exists as a unique phase in this system and that remains stable at process conditions of 115-200°C.

CHAPTER 1

INTRODUCTION

1.1 Origin of Sodium Sulfate Dicarbonate

The crystal species formed during the evaporation of a solution of sodium carbonate and sodium sulfate are identified as thermonatrite ($\text{Na}_2\text{CO}_3 \cdot \text{H}_2\text{O}$), burkeite ($\sim 2 \text{ Na}_2\text{SO}_4 \cdot \text{Na}_2\text{CO}_3$), sodium sulfate dicarbonate ($\sim 2 \text{ Na}_2\text{CO}_3 \cdot \text{Na}_2\text{SO}_4$), sodium sulfate (Na_2SO_4) and anhydrous sodium carbonate (Na_2CO_3) depending on the solution composition and temperature (Shi and Rousseau, 2001 *Crystal*; 2003 *Structure*). Concentration of spent pulping liquors in pulp and paper industry evaporators is one major industrial process that suffers from costly deposition of these salts as scales. Two double-salt species, burkeite and sodium sulfate dicarbonate were found to be the major crystal types in these concentrators.

This species was denoted as “dicarbonate” up until this work. The name sodium sulfate dicarbonate is suggested to represent the composition of double crystals that typically form with two molecules of sodium carbonate and one molecule of sodium sulfate.

Sodium sulfate dicarbonate phase crystals were predominantly found from evaporative crystallization of salt solution when the mole fraction $x = \text{CO}_3^{2-} / (\text{CO}_3^{2-} + \text{SO}_4^{2-})$ of the liquid phase was in the range $0.833 < x < 0.889$ (Shi and Rousseau, 2003 *Structure* p. 6934). Sodium sulfate dicarbonate was distinguished from burkeite by substantially higher carbonate content and a unique x-ray diffraction pattern.

Spent pulping liquors in pulp and paper industry evaporators contain various organic and inorganic materials that interact in complex ways, making it difficult to predict the influence of these materials towards the growth of double salt crystals.

Calcium ion impurities in the solutions were found to have a significant role in nucleation, growth and metastable limit in crystallization of these double salt species.

1.2 Hypotheses and Problems

Sodium sulfate dicarbonate crystals composition varies slightly with the solution composition, as does burkeite. The change of the solution composition due to crystallization or change of liquid phase composition towards equilibrium will affect the final composition of sodium sulfate dicarbonate crystals. This behavior raised questions whether the sodium sulfate dicarbonate is a transient (metastable) species that can transform to a different species. Hypothetically, if sodium sulfate dicarbonate is not stable, a change in chemical composition or temperature in the system may lead to degeneration of the crystal phase. If the sodium sulfate dicarbonate is stable, the crystal phase will remain the same over a long period of time when aged in equilibrium with the saturated mother liquor.

There have been no available data on sodium sulfate dicarbonate crystals characteristics that can be assessed to answer the problems except for the dimensions of the agglomerated forms. Sodium sulfate dicarbonate from previous works by Shi (2002) and Euhus (2003) was always found as agglomerated crystals. Hence, there has been no suitable sample that can be characterized by means of single-crystal x-ray diffraction for crystallographic properties.

Calcium ions impurities in the solutions were found to have a significant role in promoting the growth of large burkeite crystals (Shi et al., 2003 *Effects*); it may be

possible that the same impurities have the same impact on sodium sulfate dicarbonate and can be utilized in order to achieve larger crystal size which can be analyzed further.

1.3 Objectives

The purpose of this work is to contribute to the understanding of the double-salt structures and their properties in an aqueous Na_2CO_3 - Na_2SO_4 - H_2O system. In early work, the double salts isolated from mother liquor were observed to be partially changed or contaminated with different phases during prolonged exposure to ambient air. The investigation continued to answer speculative concerns that sodium sulfate dicarbonate is an intermediate or metastable species that transforms into another double salt during equilibrium with its mother liquor.

This research is intended to determine if sodium sulfate dicarbonate is a stable species and can maintain its phase during change of composition, temperature or extended period of time in contact with mother liquor.

This work also investigated the effects of calcium ions towards the stability and growth of sodium sulfate dicarbonate.

CHAPTER 2

BACKGROUND

2.1 Crystallization

Crystallization in this work refers to the formation of solid from a supersaturated homogeneous solution. Industrially crystallization is a widely used solid-liquid separation and purification technique. Operational conditions largely determine product quality in terms of physical properties and purity. Producing crystals with the desired quality requires knowledge of the basic steps involved in the process such as: supersaturation, nucleation, crystal growth, aging and other secondary processes.

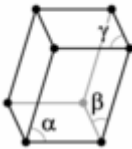
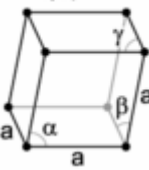
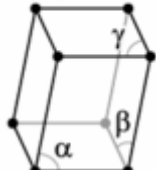
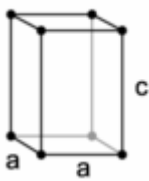
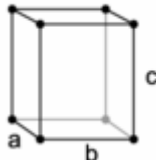
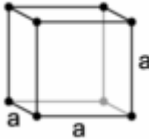
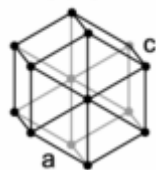
Crystallization is useful for producing solid samples from solutions, enabling atomic structure of the solids to be studied. However, production of high quality crystals has been a major challenge for x-ray crystallography.

Crystals are grown in many shapes, these shapes and aggregates can be the most important characteristics to examine when identifying organic or inorganic materials. Crystal shapes can include isometric, tetragonal, orthorhombic, hexagonal, monoclinic, triclinic, trigonal and amorphous (see Table 2.1.1).

Equilibrium in crystallization processes is reached when the saturated solution and solids composition remain constant and it can be presented in the form of a solubility curve of temperature versus solute concentration in Figure 2.1.1. This curvature is essential to identify the relationship of the saturated solution and the solids produced. In crystallization by cooling or heating, supersaturation is obtained by decreasing or increasing the solution temperature, thereby allowing the actual solute concentration to be greater than the equilibrium solute concentration. This can only happen by assuming

solubility increases strongly with decreasing or increasing temperature. In the system where the temperature is held constant, the supersaturation can instead be achieved by solvent evaporation, adding another solvent that is miscible with the solvent but has reduced solubility with the solute, or chemical reaction to form a less soluble product.

Table 2.1.1 Seven unique crystal systems from Wikipedia.org (Crystal Structure, 2006)

Crystal system	Lattices		
triclinic	$\alpha, \beta, \gamma \neq 90^\circ$ 	rhombohedral (trigonal)	$\alpha, \beta, \gamma \neq 90^\circ$ 
monoclinic	$\alpha \neq 90^\circ$ $\beta, \gamma = 90^\circ$ 	tetragonal	$a \neq c$ 
orthorhombic	$a \neq b \neq c$ 	cubic (isometric)	
hexagonal	$a \neq c$ 		

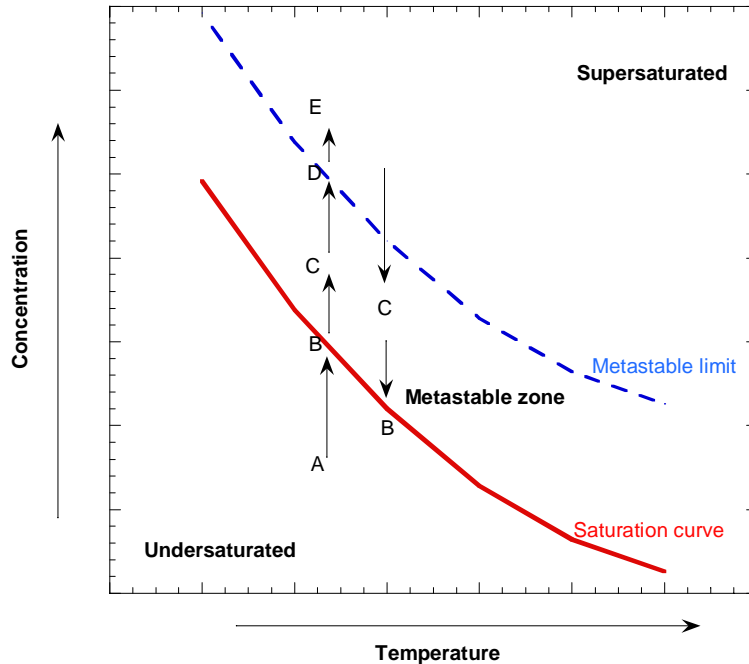


Figure 2.1.1 Zone divisions on solution system with inverse solubility.

A crystallization experiment for sodium salts such as Na_2CO_3 , Na_2SO_4 , and their associated double salts which have reverse solubility at high temperature typically begins with the solution sample in a stabilizing solution of water. Example of these salts solubility curves can be seen in Figure 2.1.2. Prior to evaporation or crystallization, this solution is undersaturated with respect to the dissolved solids. The regions where the system is undersaturated can be seen in Figure 2.1.1 at point A.

In an undersaturated solution, the solution is stable where no crystals can nucleate nor grow. Upon evaporation, the relative supersaturation of the solution moved to point B. The shift towards solubility curve can also be achieved by increasing temperature. During the increase of the relative supersaturation, several events can take place. First, in the early stage over the solubility limit, at the Metastable Zone (C), spontaneous homogenous nucleation cannot occur, but crystal growth from seeds can occur. Moving

further into supersaturation (D), the solution system entered an unstable supersaturated zone where spontaneous homogeneous nucleation and crystal growth can occur. Further into supersaturation (E), the system entered precipitation zone where precipitation of the crystals from solution also occurs.

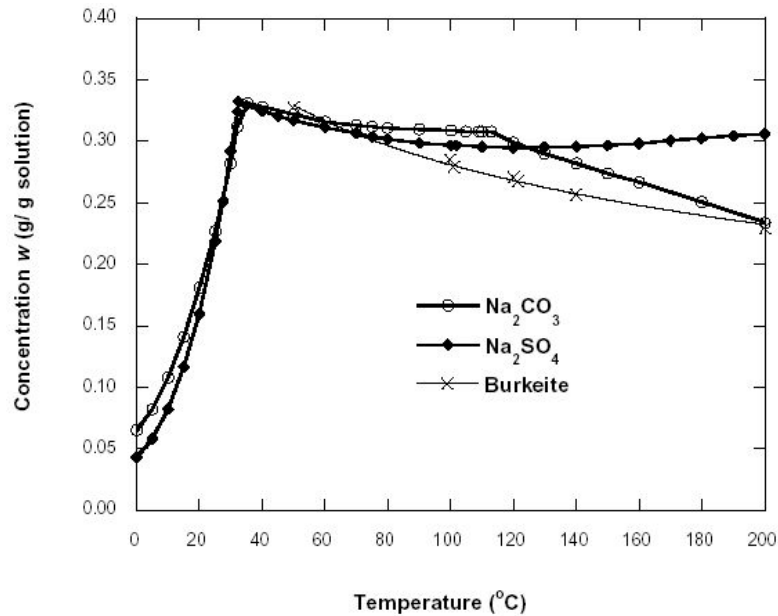


Figure 2.1.2 Solubilities of sodium salts and burkeite in water. Data adapted from Shi (2002), based on his work and various sources including Seidell and Linke (1965), Green & Frattali (1946), Frederick & DeMartini (1999).

2.1.1 Supersaturation

In order for crystallization to occur, a solution must be supersaturated. Supersaturation is the necessary driving force in which the solvent contains more dissolved solute than can ordinarily be accommodated at that particular temperature. Various techniques are used to achieved supersaturation such as by solid addition, evaporation, temperature change or antisolvent addition.

Supersaturation in a two-component system that exists in the solid and liquid phase can easily be defined as the ratio of solute species i concentration c_i and the equilibrium concentration c_i^* :

$$S = \frac{c_i}{c_i^*} \quad (2.1.1)$$

Assuming that one component crystallizes, the thermodynamic condition for equilibrium state can be expressed as the equivalent of chemical potentials of the component in both phases:

$$\mu_{1,s} = \mu_{1,l} \quad (2.1.2)$$

where μ is the chemical potential of component 1 in the solid and liquid phases. The chemical potential can be calculated from its activity α as:

$$\mu_1 = \mu_1^0 + RT \ln \alpha_1; \quad (2.1.3)$$

$$\alpha_1 = \gamma_1 c_1 \quad (2.1.4)$$

Where γ_1 is the activity coefficient and c_1 is concentration in the solution. So the potential difference of the first component at current composition with the equilibrium composition can be represented as:

$$\Delta\mu_1 = \mu_1 - \mu_1^* = RT \ln \frac{\alpha_1}{\alpha_1^*} \quad (2.1.5)$$

and the relative supersaturation can be calculated as:

$$\frac{\Delta\mu_1}{RT} = \ln S_1 = S_1 - 1 = \sigma_1 = \frac{c_1 - c_1^*}{c_1^*} \quad (2.1.6)$$

The ternary system of $\text{Na}_2\text{CO}_3 - \text{Na}_2\text{SO}_4 - \text{H}_2\text{O}$ has a more complicated equilibrium expression. Ideally, Gibbs free energies for the phase transitions are calculated on the basis of the compositions of more than one kind of mixed crystals coexisting in equilibrium with the liquid phase. For example, the equilibrium of the first component between the solid phases I and II is:

$$\mu_i^I = \mu_i^{II} \quad (2.1.6)$$

And each can be calculated as follow

$$\mu_i^{0I} + RT \ln C_i^I \cdot \gamma_i^I = \mu_i^{0II} + RT \ln C_i^{II} \cdot \gamma_i^{II} \quad (2.1.7)$$

So the potential difference which contributes to the driving force of crystallization is:

$$\mu_i^{0II} - \mu_i^{0I} = \Delta G_i^{I \rightarrow II} = -RT \ln \frac{C_i^{II} \gamma_i^{II}}{C_i^I \gamma_i^I} \quad (2.1.8)$$

Where C is the concentration of the component in mixed crystals, while different mixed crystal phases are denoted by I and II, respectively (Balarew, 2002).

Supersaturation or relative supersaturation for complex double salt species such as burkeite or sodium sulfate dicarbonate were approximated using single species

calculations in this work due to limited information from references about supersaturation or relative supersaturation of double salts species that can be applied to $\text{Na}_2\text{CO}_3 - \text{Na}_2\text{SO}_4 - \text{H}_2\text{O}$ system.

2.1.2 Nucleation

Thermodynamically supersaturated solutions will force part of the solutes to reorganize into a solid nuclei or new crystal. The nucleation from a clear solution is known as primary homogeneous nucleation and is characterized by an exponential dependence on supersaturation as well as by very large metastable zone widths (Giuletti, 2001). While primary nucleation is the creation of a nucleus in a solution with no crystals initially present, secondary nucleation requires starter crystals or “seed” to perpetuate crystal growth and initiate further nucleation.

In the primary nucleation, solute species cluster together in the solution to adopt the most efficient, lowest free energy structured arrangement of the solid state. This spontaneous nucleation is not easy to model, due to its sensitivity to the changes in the environment. Therefore, to nucleate a supersaturated solution more easily, seed crystals are often added to initiate the crystallization process which then triggers secondary nucleation. In this secondary nucleation, crystal growth is mainly initiated upon contact between the solution and seeds, thereby promoting crystallization and growth at lower supersaturation than primary nucleation required.

2.1.3 Metastable Zone

The metastable zone is the region between the solubility limit and supersaturated region plotted in Figure 2.1.1. In industrial processes, this is the region where crystallization mostly occurred. Characterizing the metastable zone gives the ability to

control, reproduce and improve the crystallization process. Crystals can grow from seeds but cannot spontaneously nucleate which is useful to control the size, preferred growth rate and the number of crystals grown.

With no clear models to follow for crystallization of double salts species from evaporation of solution containing Na_2CO_3 and Na_2SO_4 , supersaturation control should be the best way to optimize this process. This can be accomplished by studying the metastable zone width of the solubility curve as it represents the region where crystallization can be controlled.

In this particular evaporative crystallization, the width of the metastable zone can be defined as the vertical distance between the curves of the metastable limit and the solubility limit, as shown in Figure 2.1.1.

2.1.4 Crystal Growth

Crystal growth is a complex process. Supersaturated solutions are composed of a variety of units such as atoms, molecules, ions, hydrates, and clusters. Shapes and sizes of crystals can not be predicted just by knowing these variables. The driving force for crystal growth is supersaturation which controls the amount of ions in solution transported by diffusion and then built into surface of crystal, followed by reactions at the surface and then removal of reaction products from the surface. Based on this statement, crystal growth can be modeled as (1) transport-controlled growth where growth is limited by the rate at which ions can migrate to the surface via diffusion or other means of transport, and (2) surface-reaction controlled growth where growth is limited by the rate of reaction at the surface.

The growth of the crystals typically follows the repetition of unit cells in 3-D space. Crystal morphology depends upon the rate and direction in which the crystal grows, which is primarily affected by the environment conditions such as temperature,

pressure, surface shape and area where the crystal grow, and composition of the surrounding fluid which promote or inhibit crystal growth.

2.1.5 Agglomeration

Agglomeration occurs in parallel with crystal growth contributing to the size enlargement of crystals. According to Hatakka (1997), in order to avoid excessive agglomerate formation, supersaturation levels should be maintained at the lowest levels possible in the very beginning of a crystallization process.

Agglomeration strongly depends on the supersaturation and the property of the crystals, especially their affinity to adhere and form aggregates. Some agglomerations are desired since it leads to larger, easy-to-filter particles. However when the product purity is important, agglomeration should be avoided since the resulting porous structure can trap mother liquor and other impurities. The agglomeration process starts with the transport of particles towards one another. The agitation and the kinetic movement of the particles may overcome the boundary forces on the outer layer of the particles allowing them to collide and merge as agglomerate.

Most crystals observed in earlier studies of double salt crystals from evaporation of solutions of Na_2CO_3 and Na_2SO_4 are agglomerates. These double salts tend to form aggregates under the influence of reactant concentration and mixing intensity that could be proportional or inversely proportional to the agglomeration rate.

2.1.6 Crystal Aging

Crystal aging studies have been performed to examine stability of crystal systems and to improve crystal quality. Analysis of crystals kept in equilibrium with the mother

liquor for an extended period of time provides information on crystal growth or dissolution, phase changes and even crystallographic stability properties.

In general, thermodynamic stability of a solid compound arises from the ordered arrangement of its molecules in a crystal lattice in an infinite medium. For crystals with finite size, the average particle stability is an average of its volume and surface contributions. Since surfaces have a low stability due to the exposure to environment, the smaller the particle, the lower its stability. A solution with low supersaturation will consequently dissolve smaller particles. Crystal aging can take minutes, hours or even longer periods of time. Crystal aging can help to control product size and crystallinity.

2.2 Previous Research

Shi (2002) conducted evaporative crystallization experiments with aqueous solutions of sodium carbonate and sodium sulfate in the mole ratios ranging from 1:5 to 12:1. The experiments conducted at bulk conditions of 115°C within the range of 5:1 to 7:1 mole ratio of Na_2CO_3 to Na_2SO_4 lead to formation of an unknown species that was later identified as a new double salt, now called sodium sulfate dicarbonate ($\sim 2\text{Na}_2\text{CO}_3 \bullet \text{Na}_2\text{SO}_4$).

Euhus (2003) studied nucleation and growth of these crystals on heat transfer surfaces, and observed that this dicarbonate species was crystallizing at high temperature, and the scaling mechanism for surface fouling of sodium sulfate dicarbonate was adhesion followed by growth.

Several publications mentioned the formation of unique species in this solution composition range such as Helvenston et al., (1970) suggested the formula $(\text{Na}_2\text{CO}_3)_9(\text{Na}_2\text{SO}_4)_4$ on the basis of chemical analysis. Novak (1979) suggested they might be $3\text{Na}_2\text{CO}_3 \bullet \text{Na}_2\text{SO}_4$ or $\text{Na}_2\text{CO}_3 \bullet \text{Na}_2\text{SO}_4$ based on the abnormal peaks in XRD

pattern and chemical analysis. Shi, Rousseau, Euhus and Frederick built base knowledge for this species with their publications in 2001, 2003, and 2004.

Shi and Euhus speculated in their work that the dicarbonate structure is a metastable species because the crystal decomposed and its phase changed during extended period of time in storage at room temperature.

According to a series of tests performed by this group with EDTA added as a calcium scavenger. With the Ca^{2+} ions sequestered by EDTA, the aqueous salt solution of Na_2CO_3 and Na_2SO_4 exhibited lower supersaturation at primary bulk nucleation. Shi (2002) reported that that increasing calcium level increased the inhibition and consequently the metastable limit. Euhus (2003) confirmed that the inhibiting effect of calcium was strong at high mole ratios of sodium carbonate to sodium sulfate such as 6:1 or 7:1 that calcium influenced the crystallization of what was believed to be dicarbonate salt. This concluded that calcium acts as both a nucleation and a growth inhibitor.

Shi (2002) started the investigation of the effects of calcium and other ionic impurities on the nucleation of burkeite and found Ca^{2+} ion acts as primary and secondary nucleation inhibitor for burkeite and dicarbonate but not thermonatrite. Shi et al. (2003 *Effects*) speculated that dissolved calcium ions inhibited the formation and growth of crystal embryos in the bulk solution through lattice substitution, resulting in increased metastable limits for burkeite nucleation. In the event of uneven distribution of calcium ions among the nuclei, nuclei with insignificant calcium content would grow rapidly into large crystals because of the high prevailing supersaturation. In the cases where calcium ions were depleted or absent nucleation of burkeite followed its intrinsic kinetics and no large crystals appeared. (Shi et al., 2003 *Effects*).

Hydrothermal and crystal-phase stability have been investigated by researchers working with varied chemical systems. Ryoo and Jun (1997) investigated the hydrothermal stability of a mesoporous molecular sieve by observing changes in intensity and line shape of x-ray diffractograms while varying time and temperature. Forbes et al.

(1992) assessed the hydrate stability to dehydration of the potassium and sodium salts of p-aminosalicylic acid with a thermogravimetric method that differentiates between a weight loss due to dehydration and one due to decomposition. The thermal stability of the hydrates was considered to have a relationship with the strength of metal ion-to-water dipole bonding that is a function of the distance between the atoms. Johnson et al. (2003) observed the phase stability of cadmium arsenate salt crystals stored in the presence of atmospheric water by measuring the unit cell and the change in structure using a quantitative x-ray diffraction method.

2.3 Double Salt Crystals Stability

In the context of this work, stability is defined as the ability of the crystal species to maintain its unique phase properties during a change in solution composition, temperature, or an extended period of time in contact with the mother liquor. If the crystals are not stable under these conditions, then either a degeneration of the crystal or change in crystallographic properties is expected to occur.

2.3.1 Stability Identification

The stability of crystal samples were analyzed using available equipment at the Institute of Paper Science and Technology at Georgia Tech and the School of Biomolecular and Chemical Engineering Georgia Institute of Technology. Powder x-ray diffraction is often used to qualitatively identify the crystal phase, purity or the semi-quantitatively determine the weight fraction of constituents. In some cases, by comparing the integrated intensities of the diffraction peaks from each of the known phases, their

fraction can be identified. In addition, complex mixtures containing more than two phases also can be quantified.

Powder X-Ray Diffraction (XRD) was used to identify the phase stability of crystal species by comparing the diffractograms of various crystal samples directly from crystallizer with crystals that have been aged, treated, or stored in various temperature and time variables. A stable phase is expected to have no extinction or dislocation of diffraction peaks from each of the known phases. The X-ray diffraction pattern from these double salts can be identified in brief without additional treatment such as noise removal, background subtraction, and $K\alpha_2$ stripping. The phases in the mixture are identified by the usual matching procedures compared to The International Centre for Diffraction Data® (ICDD®) standards Powder Diffraction File™ (PDF), PDF-2 and PDF-4. On the other hand, for exact determination of the weight fraction of each phase can only be determined with proper treatments above coupled with reference intensity ratios (Chung, 1975) and absorption coefficients of integrated peaks of double salts that can only be found by first fully establishing crystallographic data.

Differential Scanning Calorimetry or Thermogravimetric Analysis identifies phase stability by examining the change in energy when the sample is heated to a certain temperature. When a substance is evaporating, the temperature will not increase until all the substance has evaporated, and the programmed controller increases the heat input as it attempts to increase the temperature. This extra heat flow during evaporation shows as a curve with a peak on the DSC plot. The area under the curve can be correlated to the latent heat of evaporation. An endothermic peak (during heating) on DSC plot indicates melting, dehydration or crystal phase change and an exothermic peak (during cooling) indicates solidification or crystal phase change. Figures 2.3.1 and 2.3.2 show DSC results of anhydrous sodium carbonate and anhydrous sodium sulfate heated to 500°C and cooled back to 50°C, both exhibit features indicating polymorphism.

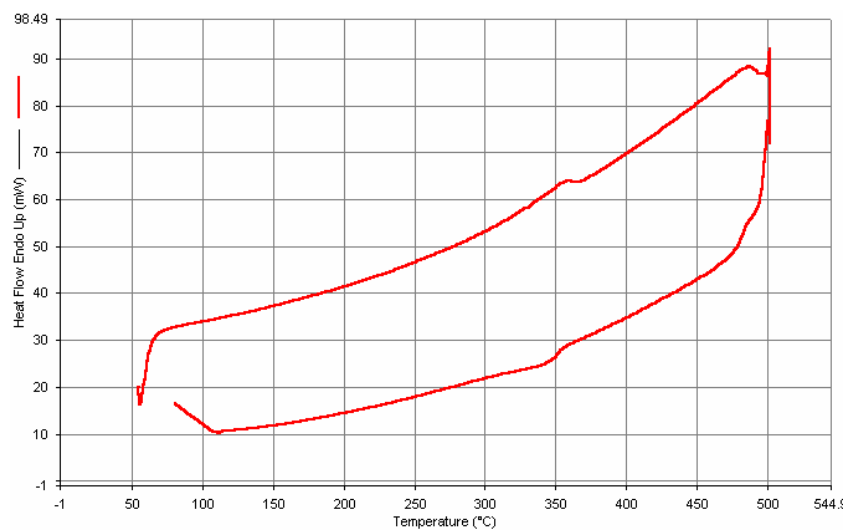


Figure 2.3.1 DSC scan of anhydrous Na_2CO_3 shows polymorph transition at 350°C

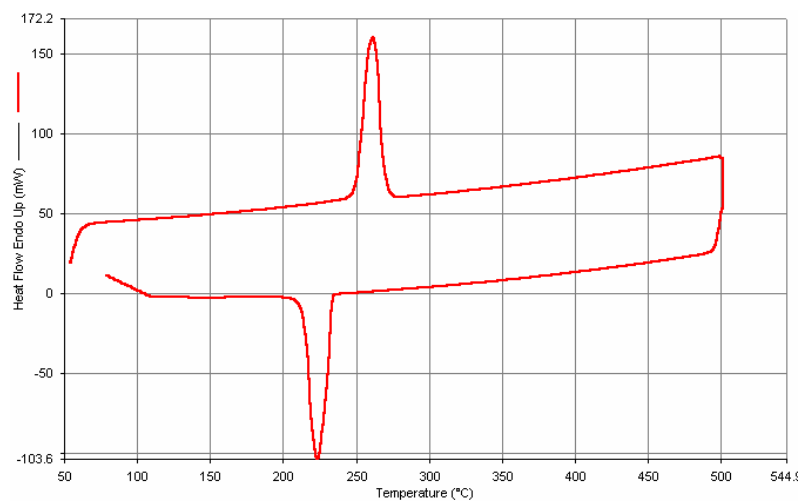


Figure 2.3.2 DSC scan of anhydrous Na_2SO_4 shows polymorph transition at 238 and 248 °C

CHAPTER 3

EXPERIMENTAL APPARATUS AND PROCEDURES

3.1 Equipments and Procedures

3.1.1 Equipments

Evaporative crystallizations were carried out in simple stirred pressure vessels of 1 and 3 liters. The schematic of both bench-scale batch crystallizers can be seen in Figure 3.1.1 and Figure 3.1.2.

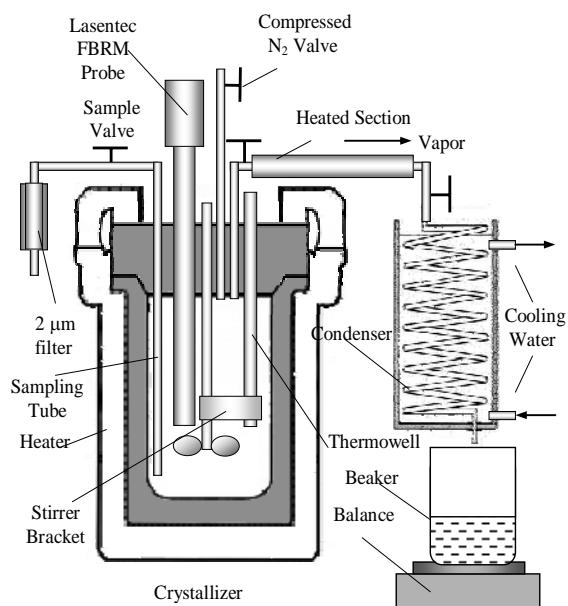


Figure 3.1.1 Schematic diagram of 1 liter bench-scale batch crystallizer

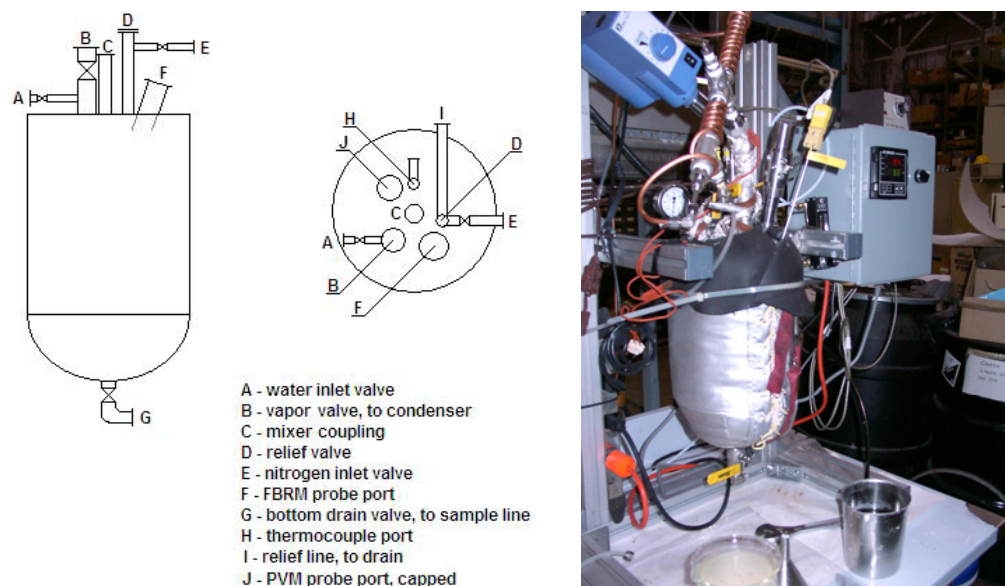


Figure 3.1.2 Schematic diagram and photograph of 3 liter bench-scale batch crystallizer

A stainless steel impeller was used as a mixer, driven by a motor with variable rotating speeds. The system temperature was controlled by a PID controller which regulates power applied to the heating jacket surrounding the vessels. Evaporated water left the vessel through a condenser and then the condensate was collected in a beaker on top of an electronic balance which is connected to a recorder so that the solids content of the residual solution could be estimated by mass balance.

For the 1 liter vessel, crystal sampling was made possible through a siphon tube (O.D. $\frac{1}{4}$ in.), with its entrance located about one centimeter above the bottom of the crystallizer, while for the 3 liter vessel, the sampling port (O.D. $\frac{3}{8}$ in.) was located on the bottom of the vessel at point G in Figure 3.1.2.

Either single crystals or agglomerates formed in the process were detected in-situ by a Lasentec® Focused Beam Reflectance Measurement (FBRM) system. A Lasentec® Particle Vision and Measurement (PVM) probe can also be used in replacement of FBRM on the 1 liter vessel, or together with FBRM in the 3 liter vessel. Using FBRM and PVM crystallization in a reactor can be monitored in real time without sampling or extracting product.

The internal pressure built during evaporation was used to force the mixture of crystals and mother liquor through a welded 2-micron in-line filter (Figure 3.1.3) which is housed in a stainless steel tube designed to handle the pressure. The filter uses porous metal filtration technology made from cleanable, 316L stainless steel filter elements which is ideal for pressure up to 14 bar, temperatures up to 400°C and highly corrosive applications. In order to isolate crystals at the process temperature, a heat tape was wrapped around the filter line and controlled to the bulk liquid temperature. Compressed nitrogen application facilitated the ability to maintain the pressure during evaporation. The system temperature, pressure, and chord counts (FBRM data) were recorded at the 10 seconds interval for first crystals experiments and 5 minutes interval or more for crystal aging experiments.



Figure 3.1.3 Porous stainless steel 2 micron filter cartridge used in crystal isolating procedures.

Approximately 800 mL of clear solution was added to the 1 liter vessel for each run as the feed and 2500 ml for the 3 liter vessel. Mixer speed was set to 250 rpm to ensure turbulence in the vessels to minimize precipitation of solids and maintain the homogeneous temperature profile in the solution.

3.1.2 Solution Preparation

Laboratory-grade Anhydrous Na_2CO_3 and anhydrous Na_2SO_4 of at least 99% purity were dissolved in deionized water to create salt solutions with 30%-dry wt. initial concentration, which is close to the solubility limits of the particular salts reported by Seidell and Linke (1965). Because calcium had been found to influence the nucleation characteristics of salts formed from such solutions (Shi et al., 2003 *Effects*), calcium content of less than 300 mg/kg in the reagents was noted.

Based on the previous study by Shi and Rousseau (2001 *Crystal*), the initial molar ratio of Na_2CO_3 to Na_2SO_4 in the solution is crucial to produce a specific phase of crystals. Evaporation of solution with Na_2CO_3 to Na_2SO_4 ratio of 1:2 is going to produce burkeite and 6:1 will produce sodium sulfate dicarbonate. A batch of experiments was also done using the ratio of 1:2, 6:1 and 6:1 with additional EDTA reagent in the solution. Addition of EDTA creates a complex with Ca^{2+} so the burkeite or sodium sulfate dicarbonate can crystallize freely without inhibition (Frederick et al., 2004). An excess EDTA in the amount of 1000 mg/kg of solution was added to this solution. The solutions were continuously mixed in a beaker for 30 minutes to ensure that all solids were dissolved before adding to the reactor.

3.1.3 Evaporative Crystallization

The reactor was sealed and the mixture heated to 115 °C before the vapor valve was opened. Evaporations were carried out at constant rate (5 g/min) at 115 °C to reach nucleation, which was defined as corresponding to more than 2000 chords count per second in the FBRM-measured size range 9 to 100 μm . The FBRM was kept online throughout the evaporation and crystal aging experiment our monitoring the chord lengths of crystals suspended in the solutions which provided information about crystal population.

To reduce agglomeration in some experiments, the evaporation was stopped before nucleation was detected by FBRM. According to Hatakka (1997), lower supersaturation reduces agglomeration. This promoted secondary nucleation and growth instead of rapid unpredictable primary nucleation at high supersaturation level.

Evaporation was then stopped and the sample was collected through a preheated, insulated 2-micron in-line filter. The mother liquor was collected into a known volume of dilution water and the crystals were rinsed sequentially using 100 ml of 1:1-volume mixture of water and ethylene glycol at 45 to 50°C, and then, at room temperature, 100 ml ethylene glycol, followed by two batch of 100 ml ethanol. Solvents are drawn through the filter cake by means of a vacuum pump connected at the end of the system. Air was allowed to flow through the filter before and after each of the solvents. The crystals were then removed from the filter chamber and stored in an evacuated desiccator.

This solvent rinse protocol is similar to what Shi (2002) suggested to remove residual mother liquor from the crystals and avoid bridging and formation of contaminant crystal phases during isolation. The water-ethylene glycol mixtures were used to reduce the activity of residual mother liquor and prevent the precipitation that can lead to crystallization of salts inside the filter. The ethanol was then used to remove the ethylene glycol residue in sample. The sodium salts in pure ethylene glycol have very limited solubility, but they are quite soluble in ethylene glycol-water mixtures (Vener, 1949; Oosterhof, 1999). Mixing the $\text{Na}_2\text{CO}_3 - \text{Na}_2\text{SO}_4 - \text{H}_2\text{O}$ solutions with a proper mixture of ethylene glycol and water could avoid the precipitations of these salts (Shi, 2002).

During crystal aging experiments, after the evaporation was stopped and a crystal sample at time equal 0 hour was isolated, pressure and temperature of the system must be checked and additional N_2 gas may be added to achieve the desired condition.

Early works in which this procedure was developed, suggested that any exposure of saturated solutions rich in Na_2CO_3 and at temperatures below 109 °C (e.g., a cold filter

housing) must be avoided to prevent $\text{Na}_2\text{CO}_3 \cdot \text{H}_2\text{O}$ formation during crystal sampling and isolation.

3.2 Analysis Methods

3.2.1 Particle Vision and Measurement (PVM) and Focused Beam Reflectance

Measurement

Lasentec® D600L (FBRM) and PVM700 instruments were used to monitor crystallization in the batch evaporative crystallizers. FBRM was used to trend chord length distribution during evaporation. Because the salt solutions reached supersaturation, crystals began to form. Nucleation was detected by FBRM as a sudden increase in the chord counts of the fine particles.. As the process continued, the counts of larger particles also increased denoting the growth of crystals in the crystallizer.

The FBRM probe was configured to detect the start of nucleation by using F (fine) tuning instead of C (coarse) to improve fine particle recognition of nuclei ore ($<< 100 \mu\text{m}$) and improve identification and measurement of primary nucleation.

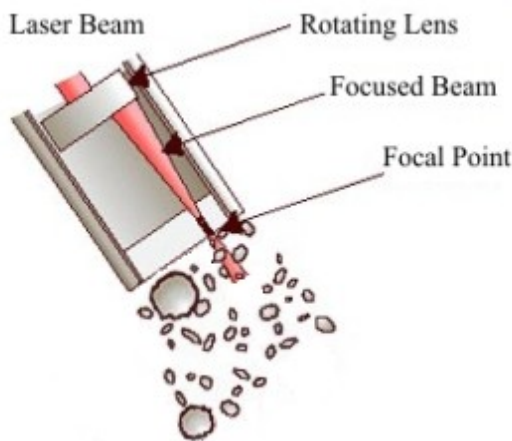


Figure 3.2.1 Simple schematic representation of the tip of the Lasentec® FBRM probe

PVM images were taken just before the nucleation started until the images were blurred by a layer of salt scale that formed on the cooled optical lens of the PVM. Both FBRM and PVM could be successfully used to identify the nucleation point and the growth of the particulates.

3.2.2 Powder X-Ray Diffraction (XRD)

The stability of crystals samples was investigated by following the change in intensity and specific peak location on diffractograms as a function of time and temperature. The crystals were ground and analyzed using a Philips® PW1710 automatic powder diffractometer with a Cu anode with APD 3720 and PANalytical X'Pert HighScore Plus analysis software.

Shi (2002) and Euhus (2003) investigated the difference of these XRD patterns for each sodium salt species and used this information to define the crystal regions of the various species during evaporation of Na_2CO_3 and Na_2SO_4 salt solutions. The XRD patterns for each species appeared to be unique, distinguishable visually, and match the standards from ICDD® standards PDF® except for sodium sulfate dicarbonate that is still unlisted.

XRD results from this work were investigated at lower diffraction angle ($2\theta < 40$ degrees). Appendix B consists of these XRD results in comparison with the standards up to 70 degrees of diffraction angle.

3.2.3 Differential Scanning Calorimetry (DSC)

Thermal properties were evaluated with a Pyris 1 differential scanning calorimetry (DSC) from PerkinElmer (see Figure 3.2.2). The DSC measures the amount of energy (heat) absorbed or released by a sample as it is undergoing a programmed

temperature change in an inert atmosphere as it is heated, cooled, or held at a constant temperature. Exact 10 mg samples of crystals was inserted into an aluminum chamber and heated so that the temperature increased at a rate of 20 °C per minute, as the sample temperature increased from 50 °C to 300 °C under a nitrogen purge. Samples were then held for one minute at 300 °C before being cooled back to 50 °C. The energy flow was measured and plotted versus sample temperature.



Figure 3.2.2 DSC Pyris 1 from PerkinElmer

3.2.4 Thermogravimetric Analysis (TGA)

Analyses by this method were performed on a PerkinElmer Pyris 1 TGA thermogravimetric analyzer. The results were used to supplement the DSC data by verifying if any moisture or other substance evaporated during heating. The technique involves monitoring the weight loss of the sample in nitrogen as a function of temperature using an Auto Stepwise method. Similar to the DSC technique, 10-mg samples were heated incrementally from 50 to 300 °C with automatic internal weight measurement.

3.2.5 Polarized Light Microscopy (PLM)

Polarized light micrographs were obtained using a Canon CCD camera coupled to a microscope with crossed polarizers, red compensator and 4, 10, 20 and 40X objective lenses. The microscope lenses provide very little depth of field; therefore, the images are essentially two dimensional.

Crystals are classified as being either isotropic or anisotropic depending upon their optical behavior and whether or not their crystallographic axes are equivalent. Isotropic crystals with equivalent axes will interact with light homogeneously, regardless of the crystal orientation. Light entering an isotropic crystal is refracted at a constant angle and passes through the crystal at a single velocity without being polarized, this will only result an appearance or disappearance of the transparent crystal under polarized light without any change in color.

Anisotropic crystals such as thermonatrite and sodium sulfate have distinct axes which interact with light according to the orientation of the crystalline lattice (angle) with respect to both the first polarizer lens and second polarizer lens (analyzer). Non-equivalent axes caused refraction of light into two polarized rays which travel at different velocities. Generally, at the 45-degree position, the crystal is at the optimum angle with respect to both the polarizer and analyzer to display maximum birefringence (double refraction). An example of the PLM technique for thermonatrite can be seen in Figure 3.2.3.

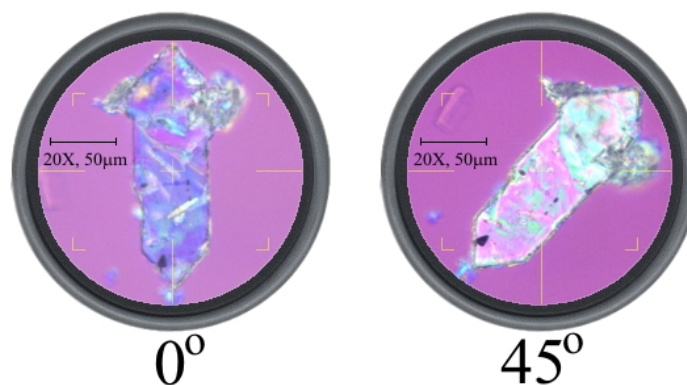


Figure 3.2.3 Polarized light micrograph of a single $\text{Na}_2\text{CO}_3 \cdot \text{H}_2\text{O}$ (Thermonatrite) crystal shows maximum birefringence at 45° rotation.

Visually seen colors and shapes can be used to identify crystals and differentiate crystal thickness. Structural changes may lead to visual changes in the shape, color or optical properties of the crystals.

3.2.6 Thermal Exposure

Crystal samples were exposed to high temperature (200°C) in an air-drying oven for one hour and then reanalyzed to observe if any changes took place. The exposure to heat will evaporate any residual ethylene glycol and ethanol solvents from the crystals isolation procedure. The dried crystals were retained in an evacuated desiccator and examined rapidly before any changes could occur by moisture absorption.

CHAPTER 4

RESULTS AND DISCUSSION

4.1 Development of Crystal Isolation Procedure

The first crystallizer used in this work has a capacity of 800 ml of solution. This 1-L vessel is equipped with only one probe port, normally used for FBRM to detect the nucleation. Multiple sampling was limited to 3 times in this system in order to maintain liquid level above the probe tip and to isolate enough crystals for analysis. Each crystal harvest will increase the risk of sample port blocking by scaling and reduced the total volume of the solution in the crystallizer. A newer apparatus become available with higher capacity of 2800 ml of solution. This 3-L bench top reactor is equipped with 2 probe ports for both FBRM and PVM that can be used simultaneously during the evaporation process. Extended runs for crystal aging experiments with more than 3 harvests can be performed in this vessel with lower risks of sample port blocking, and dropping liquid level below the probe tips. The new crystallizer also had better temperature control and safety features to allow unattended operation.

Sufficient turbulence inside the vessel is required to minimize precipitation that may block the sample port or form scale on the heated wall surface. According to equation 4.1.1, the approximate the Reynolds Number (N_{Re}) in relationship to mixer impeller rotation, more than 15 rpm is needed to reach N_{Re} above 2000. The effects of probes inserted in the liquid and mixer blade shape were not considered in this approximation, so more than 200 rpm was used in the experiments, which is more than

enough to achieve a proper mixing without plugging. This highly turbulent flow may result in crystal breakage and promote agglomeration.

$$N_{\text{Re}} = \frac{D^2 N \rho}{\mu}; \quad (4.1.1)$$

Where D is the impeller diameter (0.1 m); N is impeller rotation per second; ρ is solution density (1298 kg/m³) for 30%-wt solution, μ is solution viscosity (~0.0015 Pa.s).

Two different procedures were used to initiate crystallization. The first method is to maintain steady evaporation to high supersaturation until massive spontaneous nucleation occurs. Crystals were harvested after the FBRM chord counts for smaller size ranges, 1-100 μm , suddenly increased and reached 2000 cps. By the end of harvesting the chord counts typically exceeded 10,000 cps. 2000 cps is a good threshold level for obtaining reproducible crystal yields (20-50 g) that do not plug the ports or filter chamber. A lower threshold level such as 1000 cps resulted less than 5 gram of sample which is inadequate for multiple component analysis.

For multiple sampling for crystal aging experiments, the first method is highly susceptible to the risk of port blocking as the solution concentration can reach more than about 5% of relative supersaturation before primary nucleation occurs and this high supersaturation can promote scaling in the sample port and pipes during the aging process.

The second method stopped the evaporation early before nucleation detected by the FBRM at solids concentration below ~5% of relative supersaturation. At this point, the solution system supposed to be at lower supersaturation compare to the one generated with the first method. By holding the temperature and pressure constant at 115°C and 30 psig, nucleation occurred around 1 hour after evaporation was stopped for solutions without additional EDTA to sequester Ca^{2+} ions and around 10 minutes after evaporation

was stopped for solutions with EDTA. The lag time between the end of evaporation and primary nucleation indicated transient nucleation kinetics took place in the system. The factors that caused this delay in primary nucleation, such as a crystallization energy barrier or formation of a transient metastable phase were not investigated in this work. The summary of these systems can be seen on table 4.1.1.

Table 4.1.1 Primary nucleation delay when the evaporation of solution with 6:1 molar ratio of Na_2CO_3 to Na_2SO_4 was stopped earlier.

Solution composition:	%-wt solids when the evaporation stopped	Time to reach nucleation after the evaporation stopped.
Solution With EDTA	32.73	10 minutes
Solution Without EDTA	33.37	60 minutes

Multiple crystal isolations in crystal aging experiments were made possible using this method with the lower risk of scale and port blocking.

A sequence of experiments was performed to evaporate water from aqueous solution of Na_2CO_3 and Na_2SO_4 at 100°C with various molar ratios (1:2 to 6:1). Crystals formed from these experiments were isolated, vacuum dried and examined by XRD to identify phases, and the results are given in Figure 4.1.1 and tabulated in Table 4.1.2. This confirmed that the evaporation of salt solutions within the specific range of molar ratios at 100°C was not successful to produce sodium sulfate dicarbonate crystals. Based on the phase transition and equilibria data of sodium carbonate, thermonatrite forms at temperature below 109°C instead anhydrous Na_2CO_3 .

These samples were then analyzed by the DSC method and the scan results in Figure 4.1.2 show that dehydration of $\text{Na}_2\text{CO}_3 \cdot \text{H}_2\text{O}$ to anhydrous Na_2CO_3 created peaks as the energy flow increased to maintain constant rate of elevated temperature.

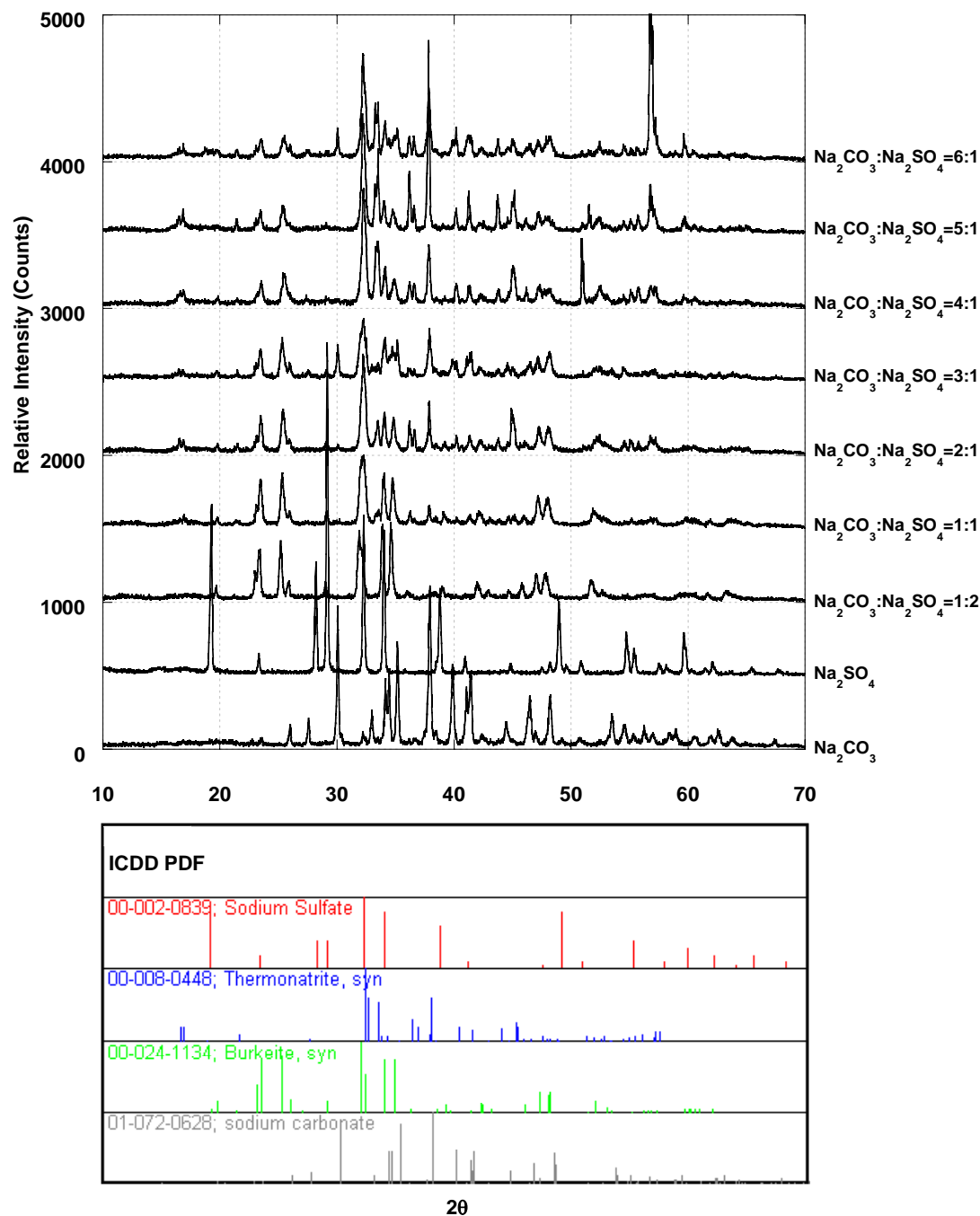


Figure 4.1.1 XRD analysis result of crystals from the evaporation of the solution containing various molar ratio of Na_2CO_3 to Na_2SO_4 at 100°C . (See Appendix B, Figure B3).

Table 4.1.2 Phase identifications from the XRD results on Figure 4.1.1

Na ₂ CO ₃ : Na ₂ SO ₄ molar ratio in initial solution	Evaporation Temperature (°C)	Crystal phase identification by XRD
1:2	100	Burkeite
1:1	100	Burkeite + Thermonatrite
2:1	100	Burkeite + Thermonatrite
3:1	100	Burkeite + Thermonatrite
4:1	100	Burkeite + Thermonatrite
5:1	100	Burkeite + Thermonatrite
6:1	100	Burkeite + Thermonatrite

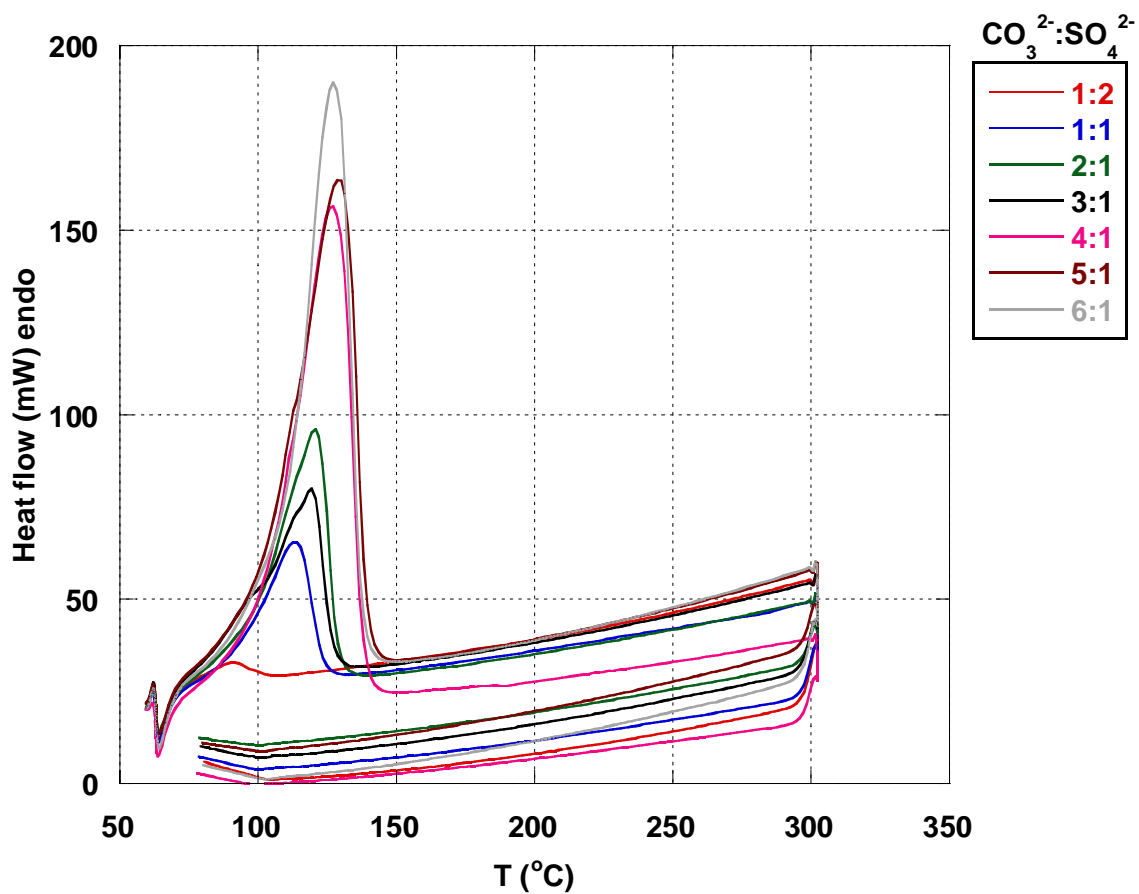


Figure 4.1.2 DSC Scan of crystals from the evaporation of the solution containing various molar ratio of Na₂CO₃ to Na₂SO₄ at 100°C.

Preliminary tests at 115°C and prior experience of Shi and Euhus indicated thermonatrite contamination in crystal samples collected from mixtures expected to form sodium sulfate dicarbonate. Apparently hydrates formed when Na₂CO₃-rich mother liquor were in contact with cold surfaces in the filter chamber which was not preheated to >110°C during early tests. So it is necessary to reduce the possibility for hydrate formation by preheating the filter chamber to the same temperature as the solution temperature before harvesting.

Experiments with the PVM show large crystal agglomerates, more than 100 µm in size, already exist at early bulk nucleation. This phenomenon can be seen in Figure 4.1.3 and 4.1.4; addition of EDTA to sequester trace amount of calcium ions apparently made a difference on large agglomerates formed soon after nucleation. Shi (2003 *Effects*) mentioned the addition of EDTA suppressed the formation of large burkeite crystals. In the experiment expected to produce sodium sulfate dicarbonate, large agglomerates having a blocky and glassy appeared at early nucleation (see Figure 4.1.3a). These crystals may form from contact of the saturated solution with dry or cooler probes and may have temporarily existed in the solution. In the evaporation with addition of EDTA, no large agglomerates were detected; instead some medium sized agglomerates were formed. These agglomerates as in Figure 4.1.4a were later identified as sodium sulfate dicarbonate.

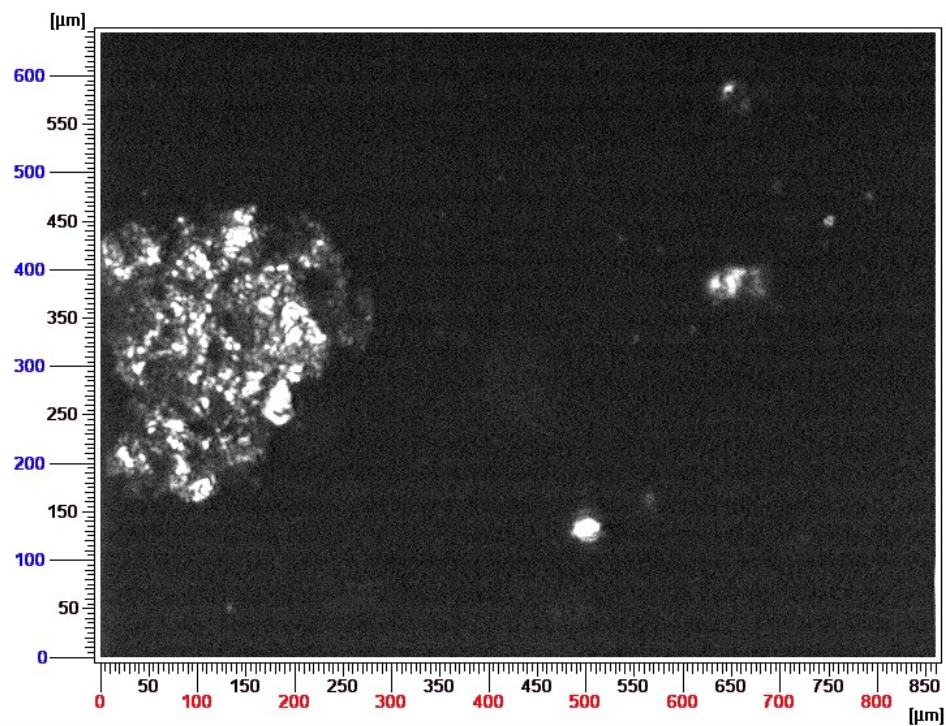


Figure 4.1.3a PVM image of crystals from early nucleation from evaporation of aqueous solution of Na_2CO_3 and Na_2SO_4 with 6:1 molar ratio at 115°C without EDTA taken at point A in Figure 4.1.3b at 2:17 PM.

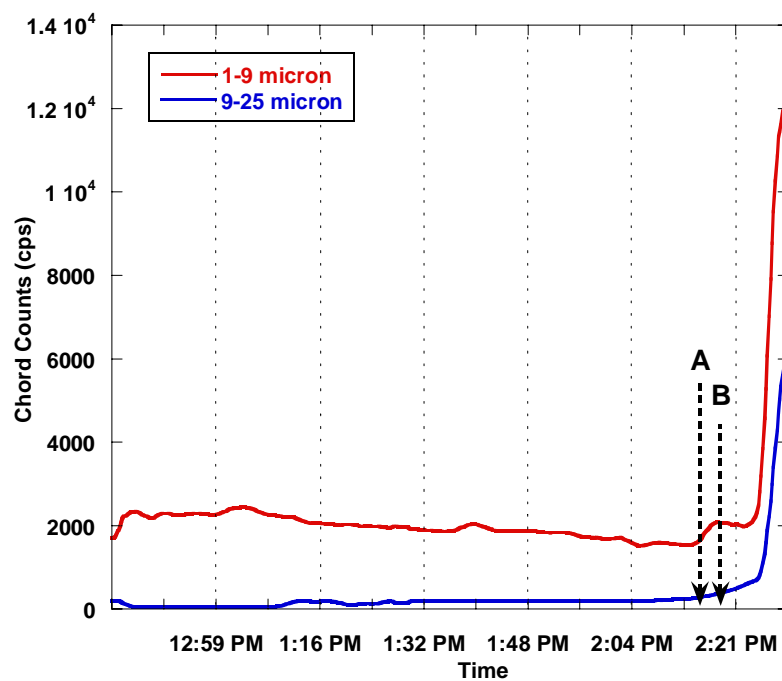


Figure 4.1.3b FBRM data for evaporation of aqueous solution of Na_2CO_3 and Na_2SO_4 with 6:1 molar ratio at 115°C without EDTA.

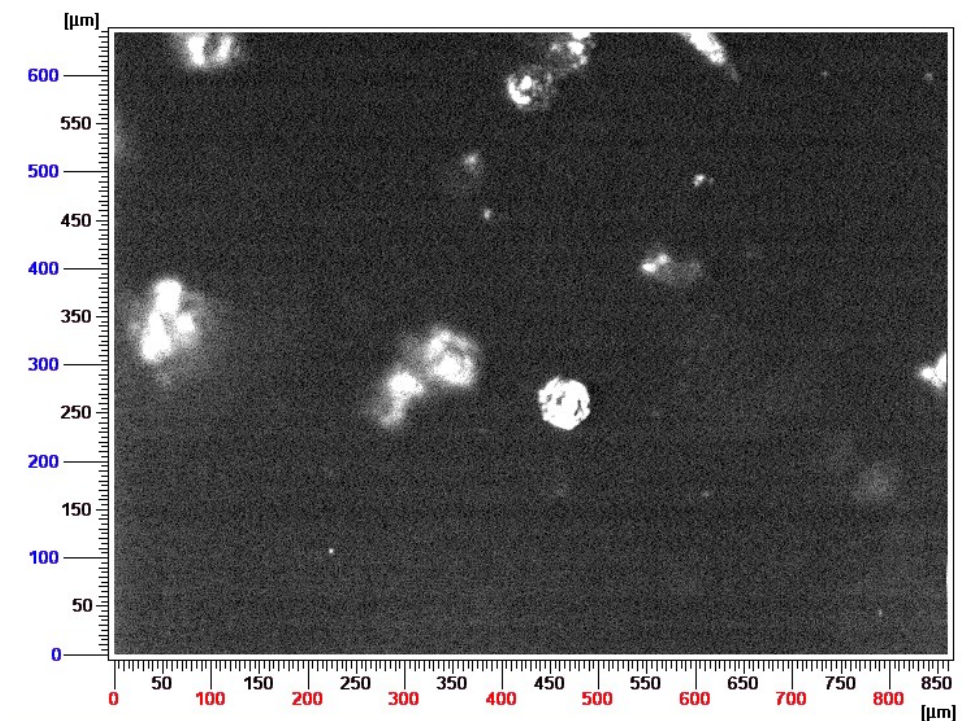


Figure 4.1.3c PVM image of crystals from early nucleation from evaporation of aqueous solution of Na_2CO_3 and Na_2SO_4 with 6:1 molar ratio at 115°C without EDTA taken at point B in Figure 4.1.3b at 2:19 PM. Some hexagonal structures appeared which later on identified as sodium sulfate dicarbonate.

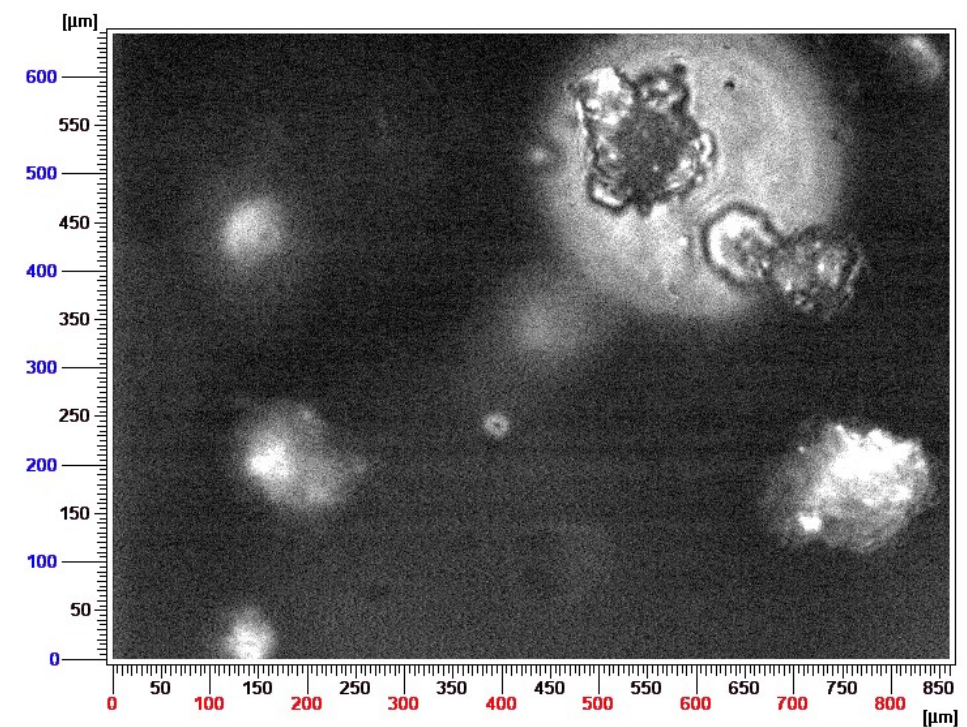


Figure 4.1.4a PVM image of crystals from early nucleation from evaporation of aqueous solution of Na_2CO_3 and Na_2SO_4 with 6:1 molar ratio at 115°C with EDTA taken at point A in Figure 4.1.4b at 10:34 AM.

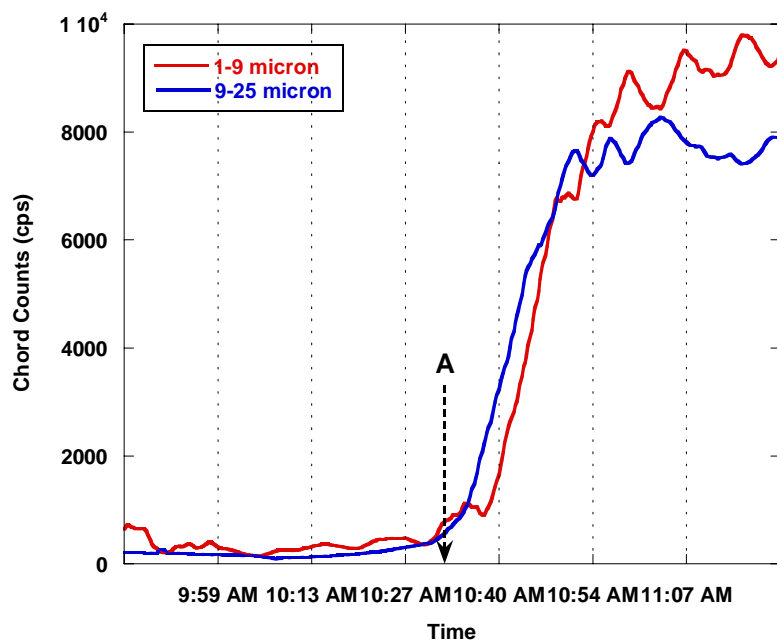


Figure 4.1.4b FBRM data for evaporation of aqueous solution of Na_2CO_3 and Na_2SO_4 with 6:1 molar ratio at 115°C with EDTA.

4.2 Stability of Sodium Sulfate Dicarboxate and Thermonatrite Crystals Mixture

Based on prior work, evaporation from of a solution containing a mole ratio of Na_2CO_3 to Na_2SO_4 in the range of 5:1 to 7:1 is expected to produce crystals of sodium sulfate dicarboxate (Shi, 2002). During some batch evaporation experiments in the present work, the evaporation was stopped after crystallization was detected (i.e., when the FBRM particle counts were greater than 2000 per second). The slurry of crystals and mother liquor were maintained in the vessel at constant temperature of 115°C and pressure of 30 psig, and crystal samples were harvested and rinsed only with ethanol after 0, 3, and 6 hours aging. Operation of the 1-L crystallizer was limited to 6 hours due to unreliable seals and lack of safety cut-offs. Figure 4.2.2 shows the FBRM data and

sampling points on the 6 hours crystal aging experiment. Based on the drop of the chords counts for 1-100 μ m, the fine crystals in the system were suspected to agglomerate and/or form scale after 4 hours in equilibrium with mother liquor. Spikes in chord counts occurred when the system was sampled.

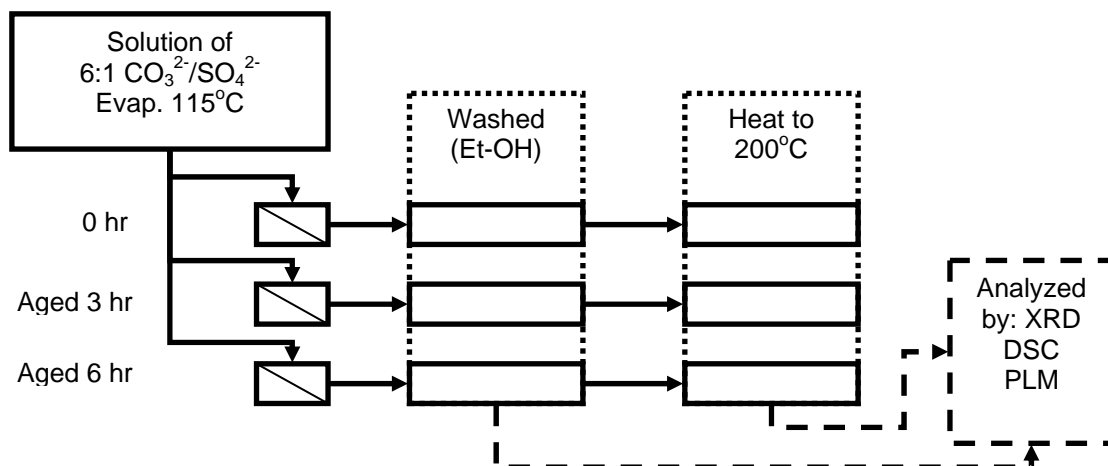


Figure 4.2.1 Experimental diagram that resulted in a mixture of sodium sulfate dicarbonate and thermonatrite crystals.

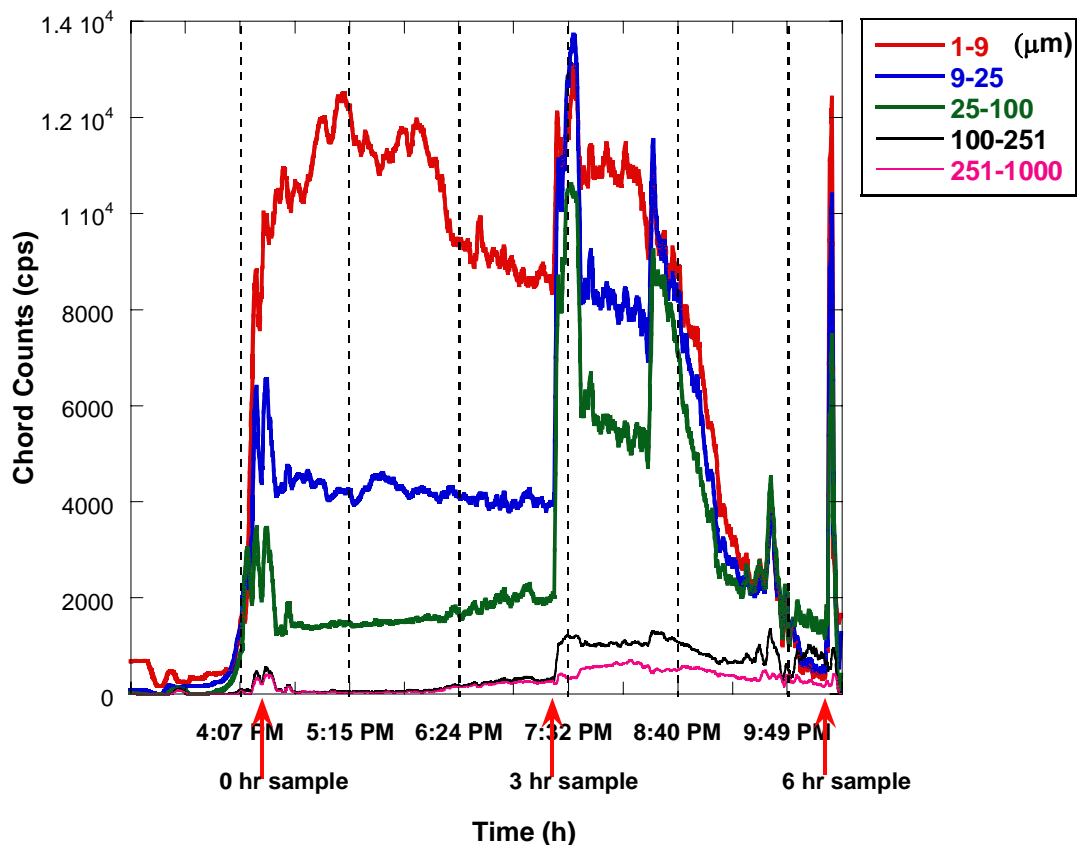


Figure 4.2.2 FBRM data for 6 hours crystal aging experiment with a solution of 6:1 molar ratio of Na_2CO_3 to Na_2SO_4 without EDTA.

It was later determined that ethanol was insufficient as a washing solvent. The ability of ethanol to reduce the water activity is not as good as ethylene glycol in a similar system (Shi and Rousseau, 2003 *Structure*; Oosterhof, 1999); hence, formation of a second crystal phase (thermonatrite) occurred during sampling. This hydrate formed when Na_2CO_3 rich mother liquor crystallized inside the filter. Thermonatrite in this sample was identified by XRD as given in 4.2.3. Peaks corresponding to thermonatrite ($\text{Na}_2\text{CO}_3 \cdot \text{H}_2\text{O}$) are apparent at 2θ of 16.7, 16.9, 21.6, 32.2, 33.6, 33.8, 34.5, 36.2, 36.6 and 38° , while characteristic peak of sodium sulfate dicarbonate appears at 20, 23.2, 23.5, 24.04, 24.5, 27.2 and 36° .

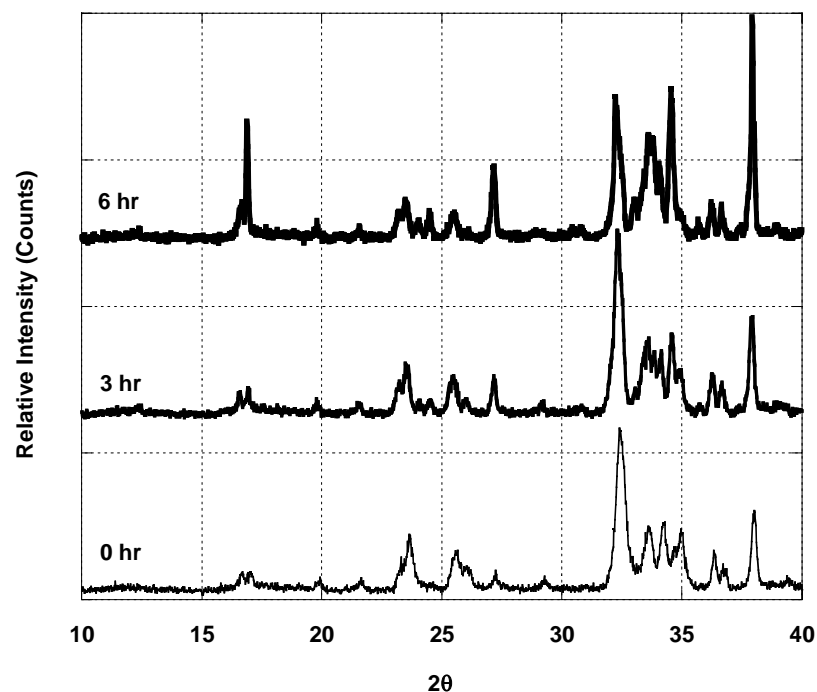


Figure 4.2.3 XRD analysis of a mixture of sodium sulfate dicarbonate and thermonatrite crystals obtained from evaporation of an aqueous solution of Na_2CO_3 and Na_2SO_4 (6:1 mole ratio, without EDTA) after aging samples 0, 3 and 6 hours rinsed with ethanol. (See Appendix B, Figure B5).

The increase intensity of the characteristic XRD peaks for thermonatrite with time on Figure 4.2.3 appears to suggest that more thermonatrite formed in the crystal-liquor slurry during aging. Note that thermonatrite may have been formed inside the filter, but the difference of the composition ratio between sample at 0 hour and 6 hours raised a question whether the structure of sodium sulfate dicarbonate evolved to accommodate more thermonatrite crystals during contact with mother liquor. Chemical analysis of the crystals at each of the recovery times was performed by coulometric titration for CO_3^{2-} content and capillary ion electrophoresis for SO_4^{2-} . These results show an apparent increase in carbonate content with aging time (see Figure 4.2.4).

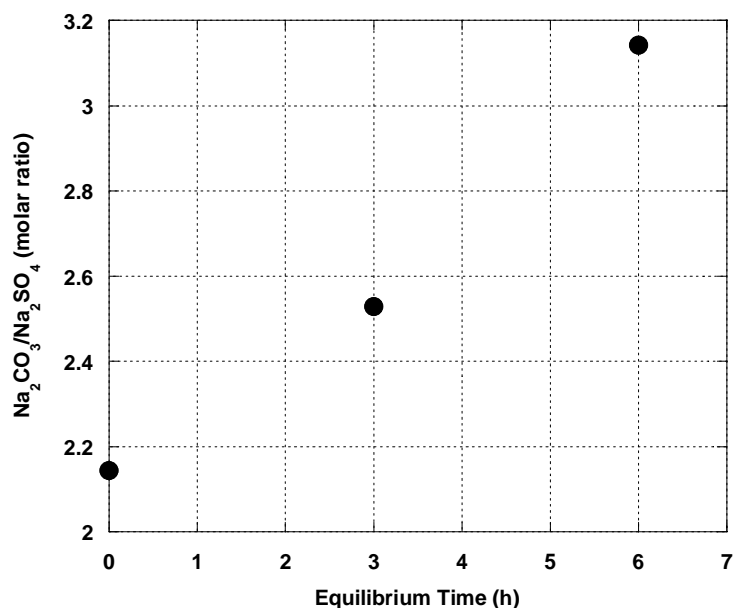


Figure 4.2.4 Chemical composition analysis of aged crystal mixtures washed in ethanol shows an increase in carbonate to sulfate ratio.

In order to confirm the presence of thermonatrite, DSC tests were performed on 10 mg of the crystals that were harvested after aging for 6 hours. The results are plotted in Figure 4.2.5. On the first scan, a significant endotherm was observed at around 78.4 °C, which is the boiling temperature of ethanol. However, the size of the peak and the change in slope as the peak rises makes it clear that the endotherm results from evolution of both ethanol and water. The first likely comes from residual ethanol on the crystal surfaces, while the latter is associated with dehydration of sodium carbonate monohydrate (thermonatrite). A similar endotherm was not observed during the second heating loop, which confirmed that the crystal sample was fully dehydrated after the first loop.

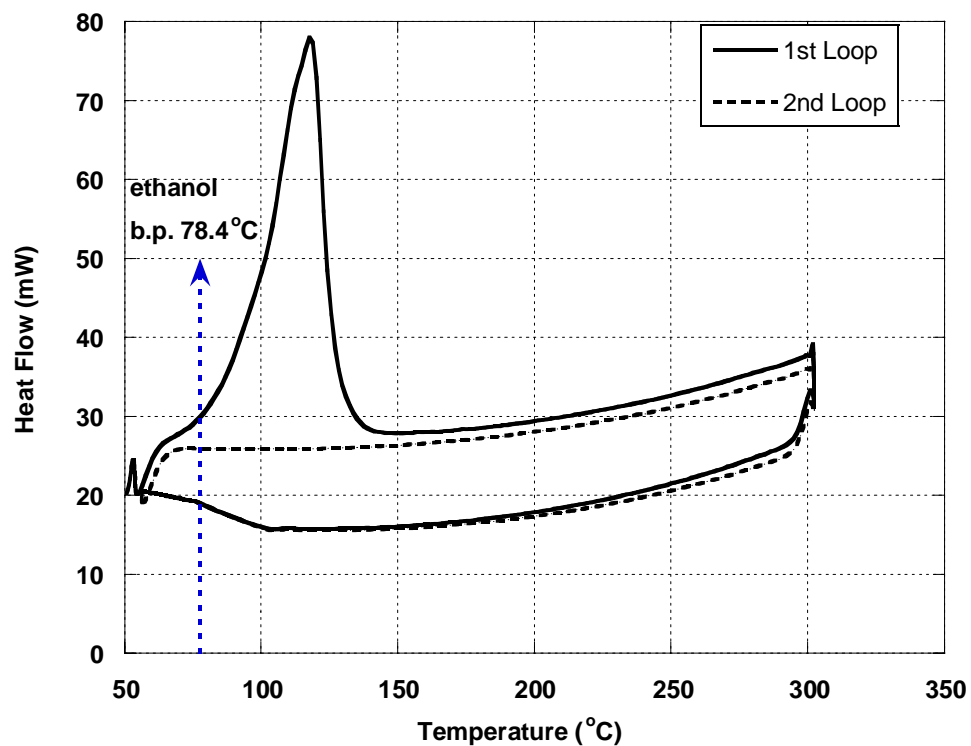


Figure 4.2.5 DSC scan of a crystal mixture sample harvested after 6 h aging showing an apparent overlap of two individual peaks in the range 78-140 °C due to evaporation of ethanol and dehydration of $\text{Na}_2\text{CO}_3 \cdot \text{H}_2\text{O}$.

The TGA scan shown in Figure 4.2.6 was obtained using a sample of the material that had been aged for 6 hours. It shows that the total sample weight decreased by about 10.2-wt %. If all of the water-mass evolved came from thermonatrite, the maximum thermonatrite content of this sample was 61-wt %.

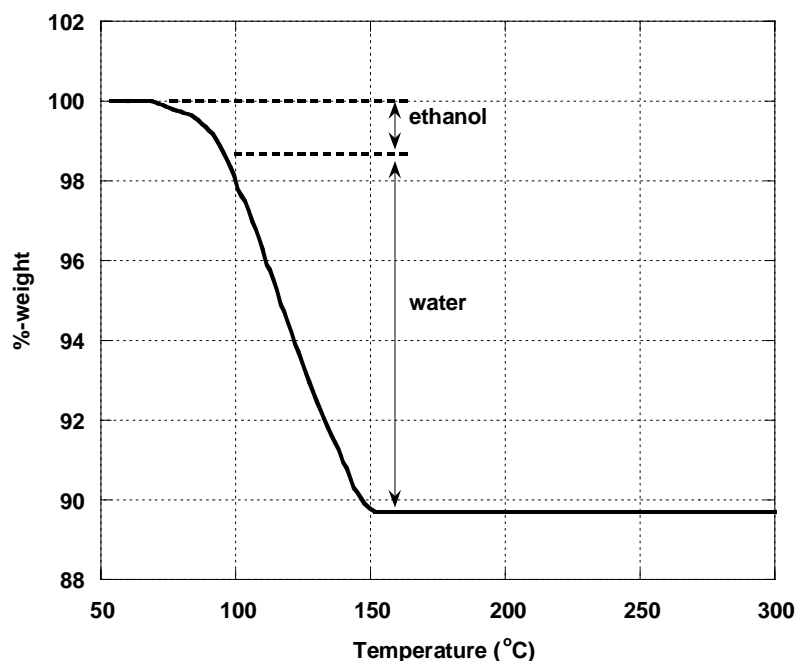


Figure 4.2.6 TGA analysis of the crystal mixture analyzed in Figure 4.2.4

Heating the mixed-salt sample to 200°C revealed a significant deformation of the structure when reanalyzed by XRD. Figure 4.2.7 shows that the specific peaks of thermonatrite were deformed and the intensity decreased significantly. This result confirms that the thermonatrite content converted to anhydrous sodium carbonate during heating. Thermonatrite peaks at 16.7° and 16.9° (A) disappeared, and the characteristic anhydrous sodium carbonate peak appeared at 30.3° (B). Sodium sulfate dicarbonate can be seen at 2θ of 23.2, 23.5, 24.04, 24.5, 27.2, 33.2, 34, 34.8 and 36°.

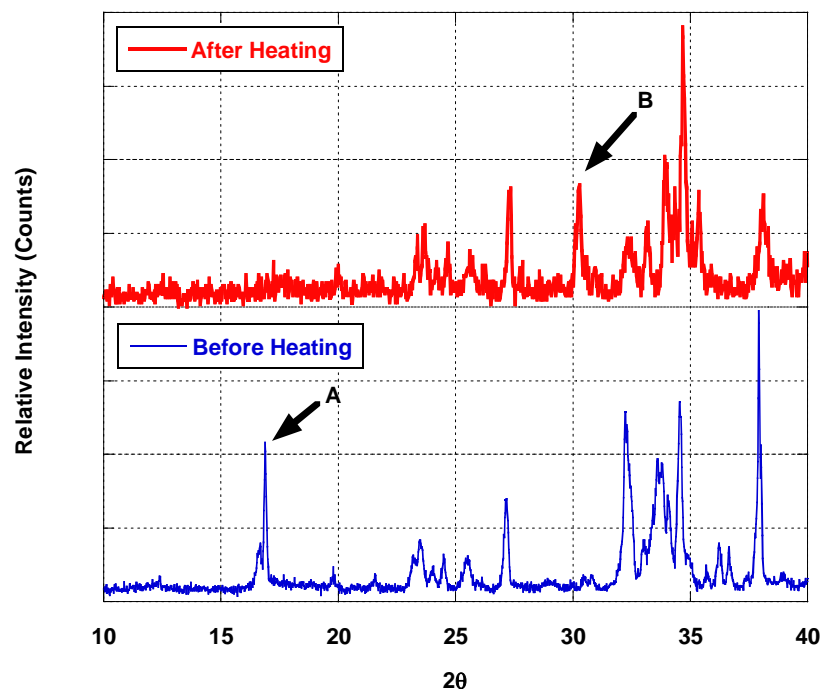


Figure 4.2.7 XRD analysis of crystal mixture of sodium sulfate dicarbonate and thermonatrite harvested after 6 h aging before and after exposure to 200 °C. (See Appendix B, Figure B6).

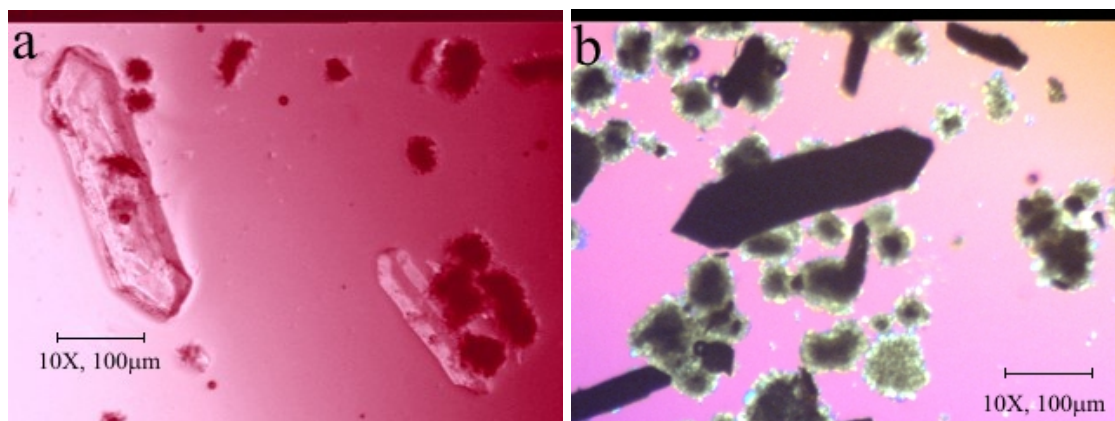


Figure 4.2.8. Photomicrographs of the sodium sulfate dicarbonate-thermonatrite mixture before (a) and after (b) exposure to 200 °C.

Dehydration of thermonatrite ($\text{Na}_2\text{CO}_3 \cdot \text{H}_2\text{O}$) also impacted the optical properties of the crystal mixture. Figure 4.2.8 shows photomicrographs of sodium sulfate dicarbonate and thermonatrite mixture before (a) and after (b) heating. Thermonatrite crystal shows as bright orthorhombic-pyramidal shapes and fragments. Thermonatrite

crystals experienced a darkening effect when dehydrated. Kim et al. (2005) also observed that dehydration reduced the transparency of crystal samples. The release of H_2O molecules created cracks and micro holes on the surface of the crystals that made impossible for light to pass through and refracted.

Note that the agglomerated, nearly spherical objects in Figure 4.2.8 are typical of sodium sulfate dicarbonate agglomerates observed in earlier studies. When harvested from solution, the mixed crystals formed are not chemically or thermally stable due to the tendency of thermonatrite to form during washing with ethanol and its subsequent dehydration when treated with heat exposure.

4.3 Thermal Stability of Burkeite Crystals

An experiment was performed using a solution with 1:2 Na_2SO_4 to Na_2CO_3 molar ratio to produce pure burkeite crystals. The crystals obtained were examined by XRD. The crystals were then heated to 200 °C and re-examined. The powder XRD results for pure burkeite crystals phase before and after heating are shown in Figure 4.3.2 over the range of 2θ from 10 to 40°. The characteristic burkeite pattern was observed before and after heating, suggesting that no transformation occurred. The peak positions and relative intensities matched the standard burkeite XRD patterns obtained by the ICDD (PDF #24-1134, 85-1731 to 85-1733, and 00-024-1134).

Evaporative Crystallization

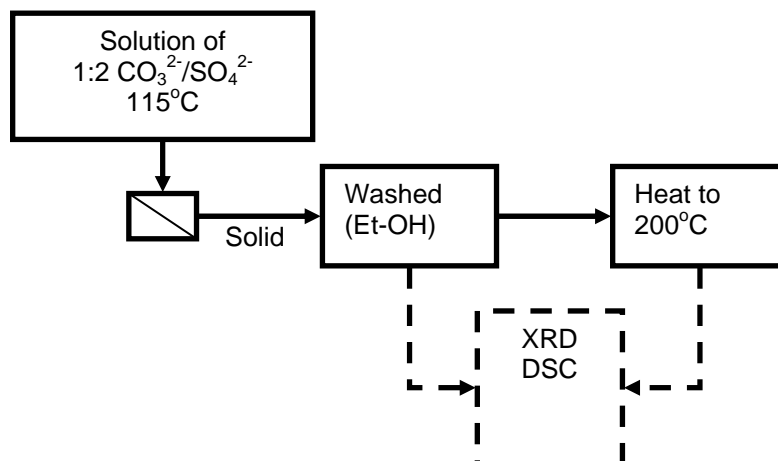


Figure 4.3.1 Experimental diagram to investigate stability of burkeite crystals.

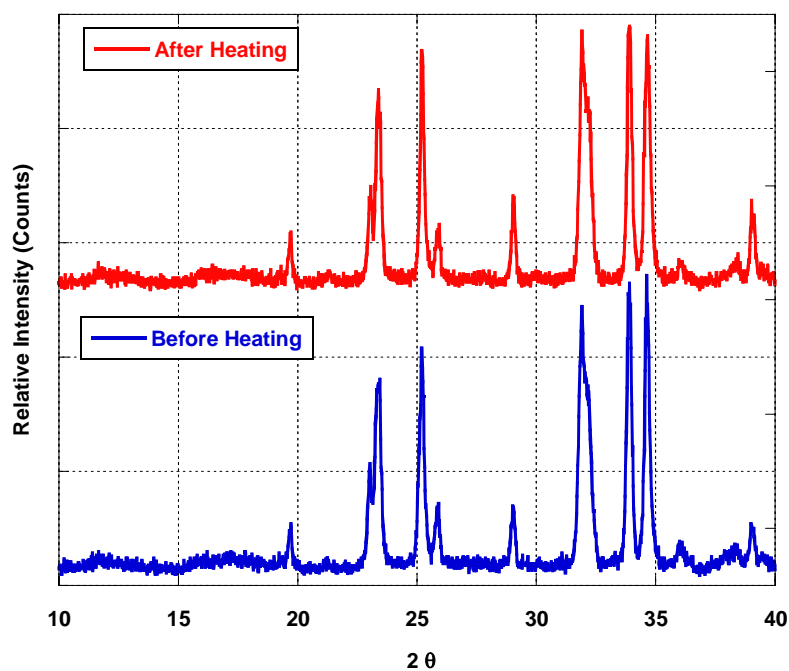


Figure 4.3.2 XRD analysis of burkeite crystals from evaporation of 1:2 molar ratio of aqueous solution of Na_2CO_3 and Na_2SO_4 before and after heat exposure to 200°C shows relatively no change in structure.

The DSC analysis shown in Figure 4.3.3 supports the conclusion that there was no transformation of burkeite during heating. The first scan (shown as the solid curve) shows that residual ethanol from the washing step was evaporated starting at around 78.4°C . Calculated area under the peak as in Figure 4.3.3 is $55.7 \text{ mW } ^\circ\text{C}$; with the heating rate of

20°C/minute and enthalpy evaporation of ethanol 838 mJ/mg, one can estimate the total heat of evaporation 169.14 mJ and the amount of the ethanol evaporated to be 1.99-wt % of the sample. The second scan (shown as the dashed curve) follows the path of the first scan except for the portion caused by evaporation of ethanol.

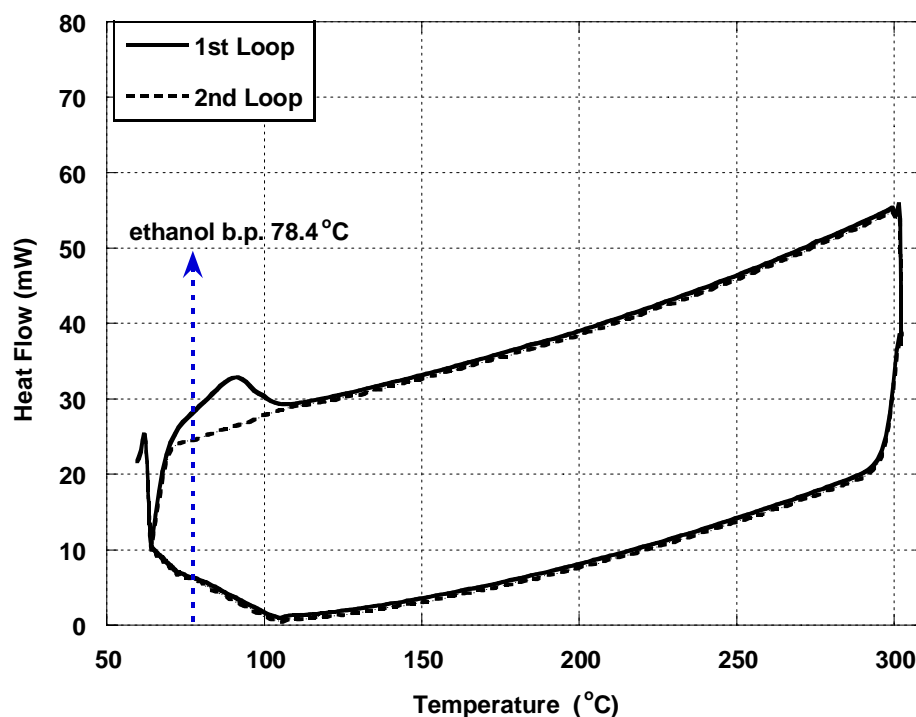


Figure 4.3.3 Two sequential DSC scans of a single sample of burkeite crystals.

This result suggests that there were no volatile impurities remaining in the sample after the first stage of heating. Furthermore, the similarity of the two scans indicates that there is no structural change in the crystalline sample, indicating that burkeite is stable and is not degenerated under this thermal exposure. These results for the well-characterized burkeite salt provide an important reference for the following discussion of the relatively unknown sodium sulfate dicarbonate salt.

4.4 Stability of Sodium Sulfate Dicarbonate Crystals

It has been discussed earlier that the introduction of EDTA into solutions of Na_2CO_3 and Na_2SO_4 apparently affected the nucleation behavior of sodium sulfate dicarbonate and burkeite. It was hypothesized that the EDTA sequestered small amount of calcium ions that came from the impurities in the reagent. Ca^{2+} ion acts as nucleation inhibitor for burkeite and dicarbonate but not thermonatrite (Shi et al., 2003 *Effects*) and the addition of EDTA kept them from interfering with nucleation and growth of crystalline species. To further evaluate this effect in the present work, solutions of Na_2CO_3 to Na_2SO_4 with mole ratio of 6:1 were evaporated using the established procedure with and without 1000mg EDTA per kg of solution added.

In the first experiment, EDTA was added in the solution before evaporation and the evaporation stopped once nucleation was detected by FBRM. The system was assumed to have reached high supersaturation and rapid nucleation occurred. Two samples were taken 0 and 24 h after nucleation was detected by the FBRM. The temperature and pressure were held constant during the aging process.

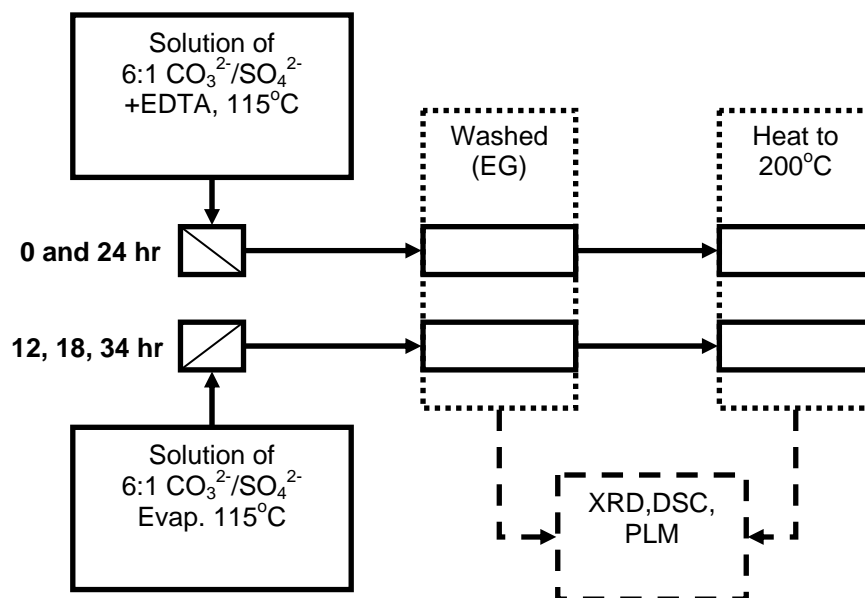


Figure 4.4.1 Experimental diagram to investigate stability of sodium sulfate dicarbonate crystals.

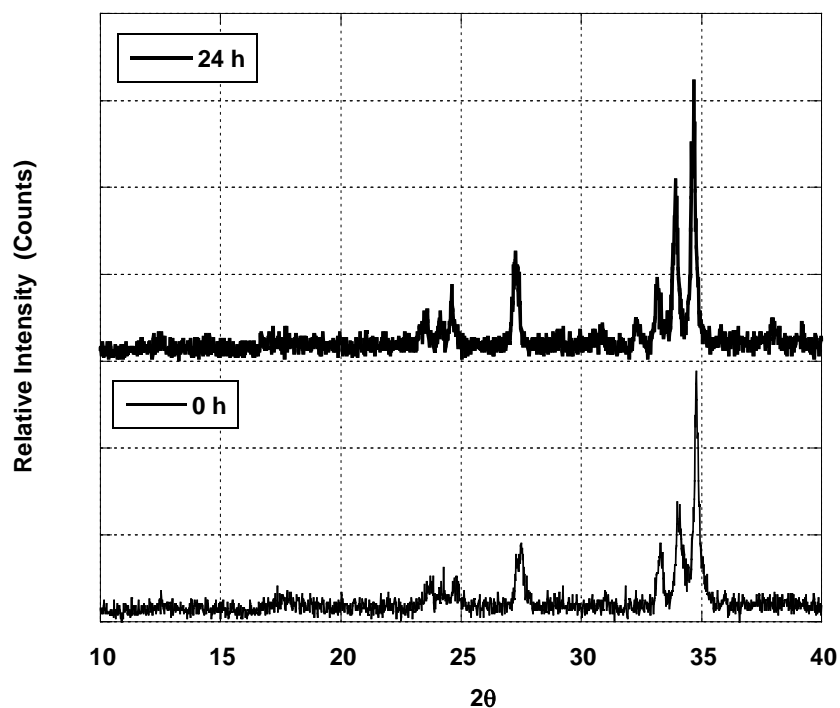


Figure 4.4.2 XRD analysis of sodium sulfate dicarbonate crystals obtained from evaporation of an aqueous solution of Na_2CO_3 and Na_2SO_4 at 6:1 molar ratio with EDTA; sampled after aging 0 and 24 hours.

The XRD results in Figure 4.4.2 confirm that a single phase of sodium sulfate dicarbonate was obtained. Apparent peaks at 2θ of 23.2, 23.5, 24.04, 24.5, 27.2, 33.2, 34, and 34.8° are the characteristic features of this salt similar to the one reported by Shi and Rousseau (2003 *Structure*). There is no loss of integrity of the sodium sulfate dicarbonate structure occurred after aging for 24 hours. It can be concluded that sodium sulfate dicarbonate is hydrothermally stable at 115°C .

Polarized light microscopy shows the structure of sodium sulfate dicarbonate crystals formed from evaporation of salt solution with EDTA as an agglomerate of crystal rods as seen in Figure 4.4.3. These rods appeared to be monoaxial similar to the crystal structure reported by Khlapova and Kovaleva (1963) for $3\text{Na}_2\text{CO}_3 \cdot \text{Na}_2\text{SO}_4$.

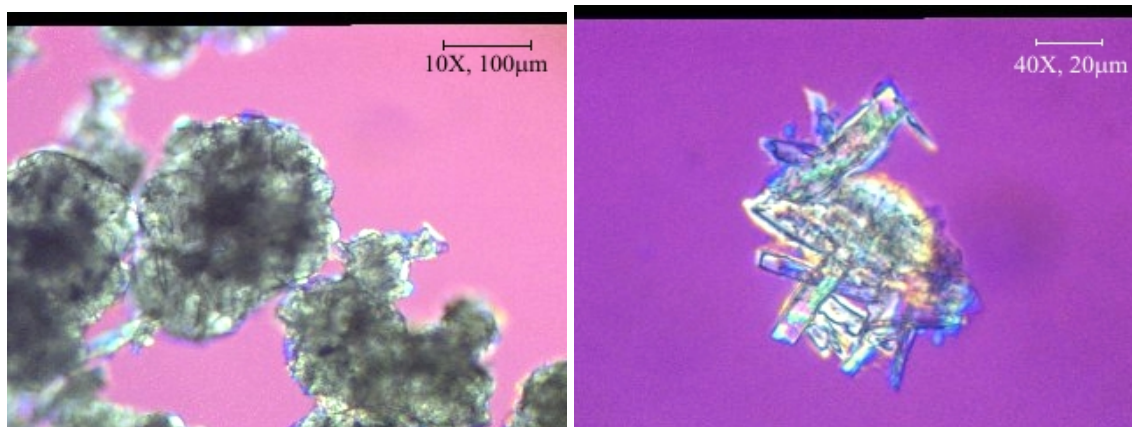


Figure 4.4.3 PLM observation on sodium sulfate dicarbonate from evaporation of salt solution with EDTA.

A crystallization experiment was done similarly to produce sodium sulfate dicarbonate without addition of EDTA in the system. The solution containing 6:1 molar ratio of Na_2CO_3 and Na_2SO_4 was evaporated at 115°C , 30 psig. The evaporation was stopped when the system reached 33.37-wt% solid, and the nucleation occurred about an hour afterwards. The system was suspected to have transient nucleation kinetics that created a lag time before primary nucleation occurred. This kinetic effect was not investigated in this work.

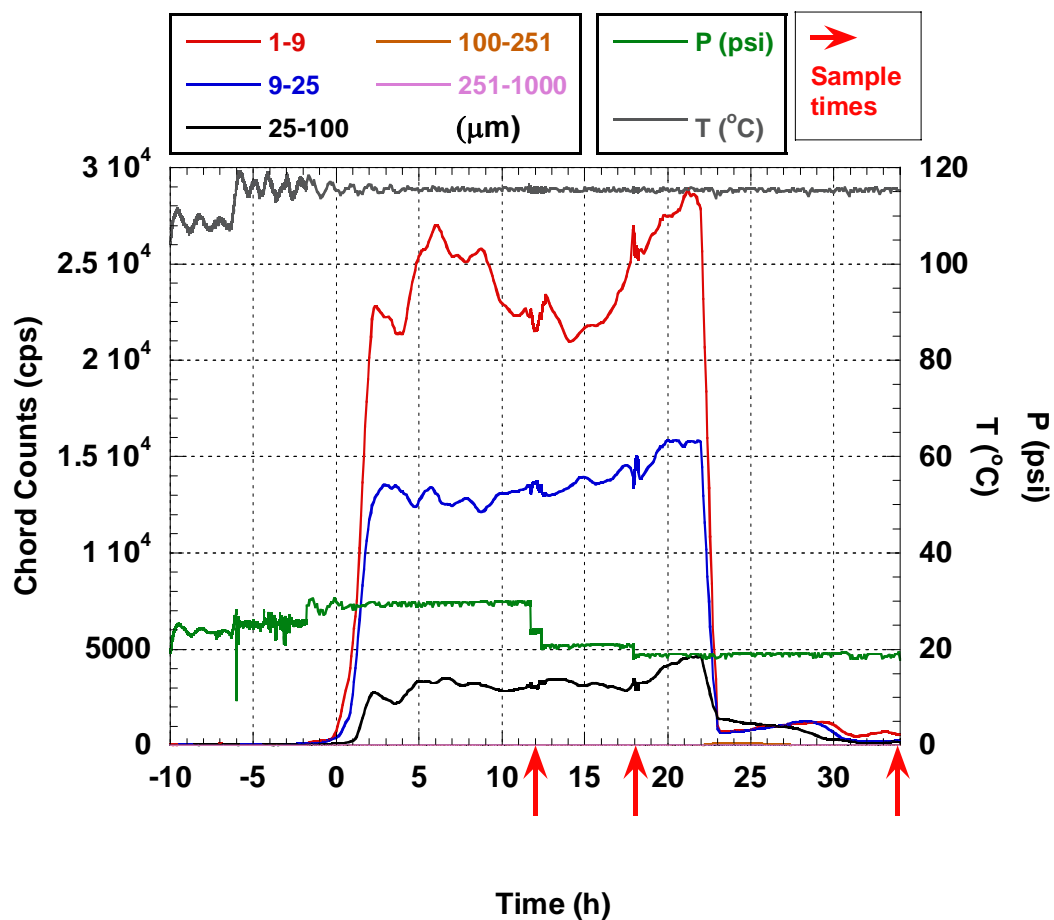


Figure 4.4.4 FBRM data during crystal aging experiment without EDTA shows chord counts, temperature and pressure measurements up to 34 hours.

During this experiment, the sodium sulfate dicarbonate crystals were aged up to 34 hours in equilibrium with the solution with relatively steady temperature and pressure. FBRM data is given in Figure 4.4.4. Crystal samples were obtained after 12, 18, and 34 hours and rinsed sequentially with the ethylene glycol-water-ethanol system described earlier. The crystals were then retained in an evacuated desiccator. Vacuum dried crystals were analyzed by powder X-ray diffraction and the result can be seen in Figure 4.4.5. Once again the characteristic peaks indicate all samples were pure sodium sulfate dicarbonate (see Appendix B). The intensity ratios between peaks were slightly different compare to Figure 4.4.2 of sodium sulfate dicarbonate produced without Ca^{2+} inhibition.

FBRM data in Figure 4.4.4 shows an apparent drop of counts at 23 hours elapsed time suggested that fine crystals were agglomerated, or deposited as scale in the crystallizer. However X-ray diffraction analysis shows no apparent transformation of the crystal phase due to this phenomenon.

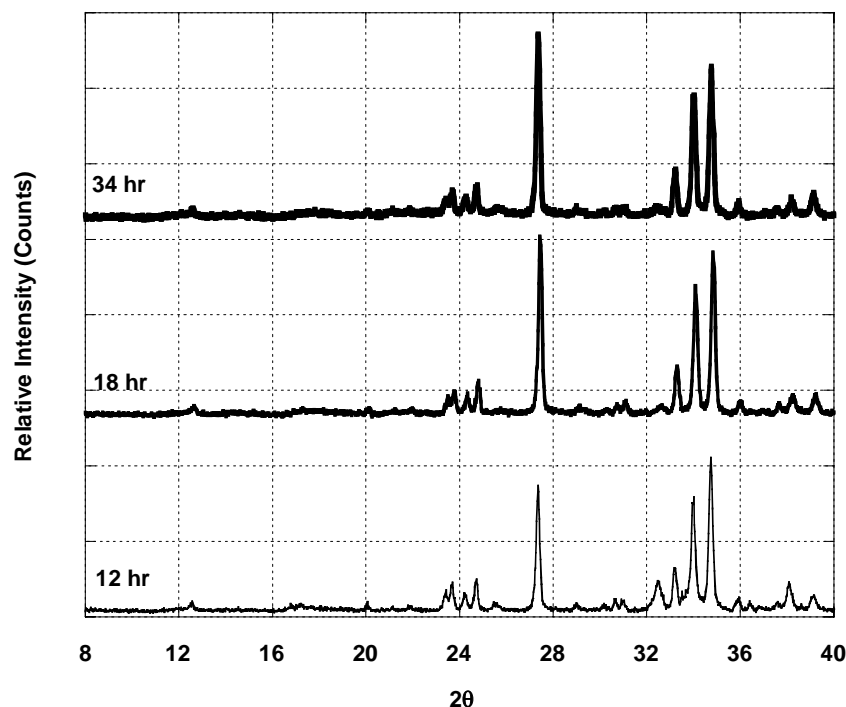


Figure 4.4.5 XRD analysis of sodium sulfate dicarbonate crystals obtained from evaporation of an aqueous solution of Na_2CO_3 and Na_2SO_4 (6:1 mole ratio, without EDTA) after aging samples 12, 18 and 34 hours (ethylene glycol + ethanol rinsed).

The composition analysis results at 12, 18 and 34 hours crystal compositions are given Figure 4.4.6. There was a change in Na_2CO_3 to Na_2SO_4 ratio in the crystals during aging. Earlier work by Shi (2002) found that aging burkeite crystals in a solution of Na_2CO_3 and Na_2SO_4 at a 1:2 mole ratio resulted in a progressive transformation of the crystal composition from a mole ratio of 0.44 to 0.50 (Na_2CO_3 to Na_2SO_4). Apparently the initially formed crystals were not in equilibrium with their mother liquor, but were transformed over time, probably in a solution-mediated process, towards the equilibrium composition. In the present case, aging the crystals in a solution with a 6:1 mole ratio of

Na_2CO_3 to Na_2SO_4 without EDTA experienced a transformation temporarily from crystals richer in sodium carbonate (having more than 2:1 mole ratio of Na_2CO_3 to Na_2SO_4) towards one that is approximately $\sim 2\text{Na}_2\text{CO}_3 \cdot \text{Na}_2\text{SO}_4$.

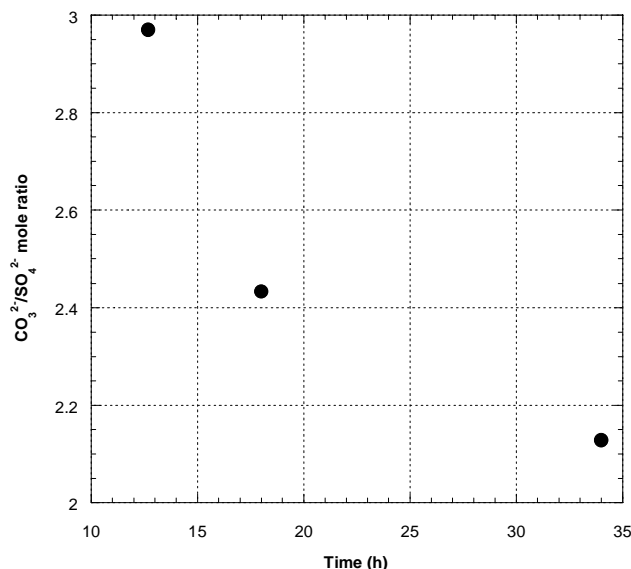


Figure 4.4.6 Transformation of crystal composition when aged in mother liquor having a 6:1 mole ratio of sodium carbonate to sodium sulfate at 115 °C.

The difference between sodium sulfate dicarbonate crystals harvested from the evaporation of solutions with and without EDTA can be observed by polarized light microscopy. In the crystal samples isolated from evaporation of salt solutions with EDTA, the only crystal habit noticed was agglomerated rod-like crystals. Crystals that were produced without the addition of EDTA shows an interesting different feature, a crystal habit that appeared as hexagonal plates growing outward from a core single rod crystal or agglomerate (see Figure 4.4.7). An experiment using the same technique with EDTA did not produce these hexagonal shapes.

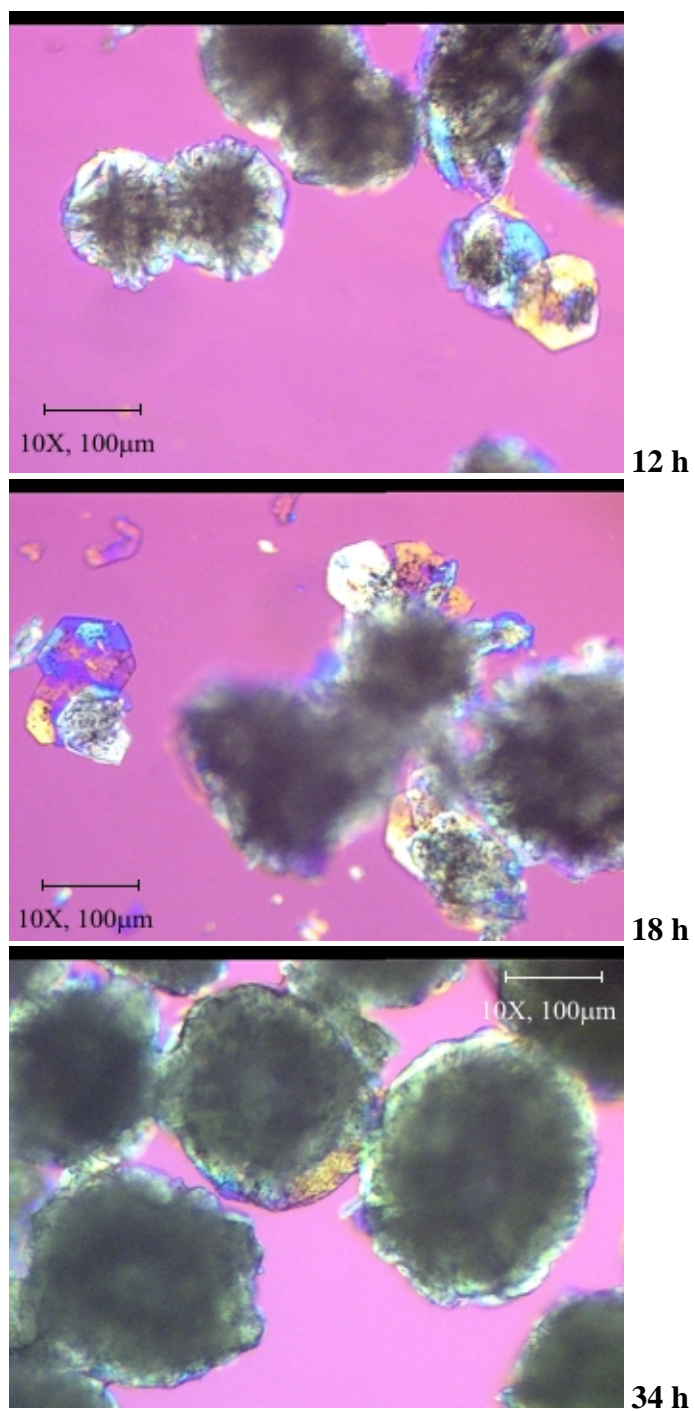


Figure 4.4.7 Photomicrographs of the sodium sulfate dicarbonate from evaporation of solution without EDTA showing coexistence of two different crystal habits, agglomerated rods and hexagonal shapes.

Possible explanations for this phenomenon are (1) hexagonal sodium sulfate dicarbonate crystals were promoted to grow by the presence of Ca^{2+} ions during

equilibrium in lower supersaturation, (2) hexagonal plate growth was inhibited by the presence of EDTA in the solution, or (3) hexagonal sodium sulfate dicarbonate is the most stable structure that formed during extended period of time in contact with mother liquor. Based on the observation through polarized light microscopy (see Appendix A) the hexagonal – bipyramidal sodium sulfate dicarbonate crystals is likely to belong to the P 6/m space group. Figure 4.4.8 shows a set of 3-D schematic representations of sodium sulfate dicarbonate in monoclinic and hexagonal shape. Note that two different hexagonal crystal planes were observed to coexist in the sample.

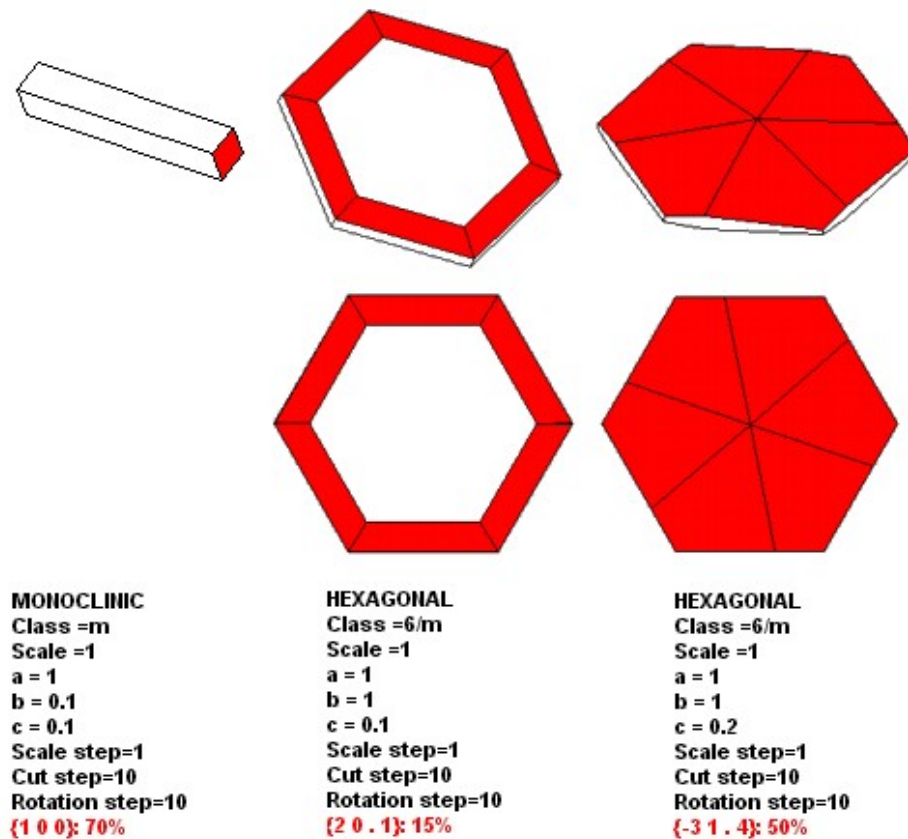


Figure 4.4.8 3-D schematic representations of sodium sulfate dicarbonate shapes based on PLM images on Appendix A. Drawn using George Favreau's FACES v.3.7 software.

Shape differences of these sodium sulfate dicarbonate crystals give some insight to internal symmetry of the crystal and relative growth rates along the various crystal axes. The presence of Ca^{2+} ions most likely promotes the growth of the crystals on its

three axes in equal rates creating a hexagonal shape. While in the system without Ca^{2+} ions the crystals grow in only one direction creating rod-like crystals. These rods will easily break and start to agglomerate. The sum of the effects by Ca^{2+} ions and low supersaturation achieved by stopping evaporation before nucleation promote the hexagonal crystal habit because this type of crystal was not detected in earlier experiments with EDTA, which were run with continuous evaporation to very high supersaturation before nucleation occurred.

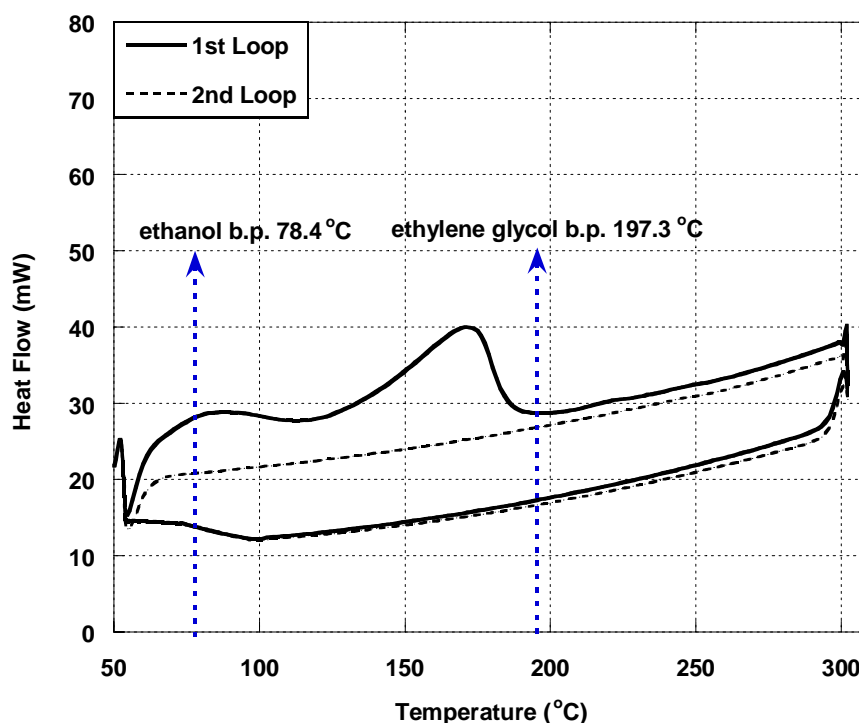


Figure 4.4.9 DSC scan of sodium sulfate dicarbonate from evaporation of the salt solution with EDTA shows features of residual ethanol and ethylene glycol (crystal washing solvent) release.

DSC results for sodium sulfate dicarbonate crystals are given in Figure 4.4.9. The small, broad peak between 78 and 108 °C is likely a result of evaporation of the residual ethanol used in crystal washing. The larger peak between 133 and 193 °C likely results from evaporation of a residual mixture of water and ethylene glycol (b.p. 197.3°C at 1

atm) that was used to displace mother liquor from the crystal sample. The second heating loop shows no peaks, confirming that the crystal sample is stable.

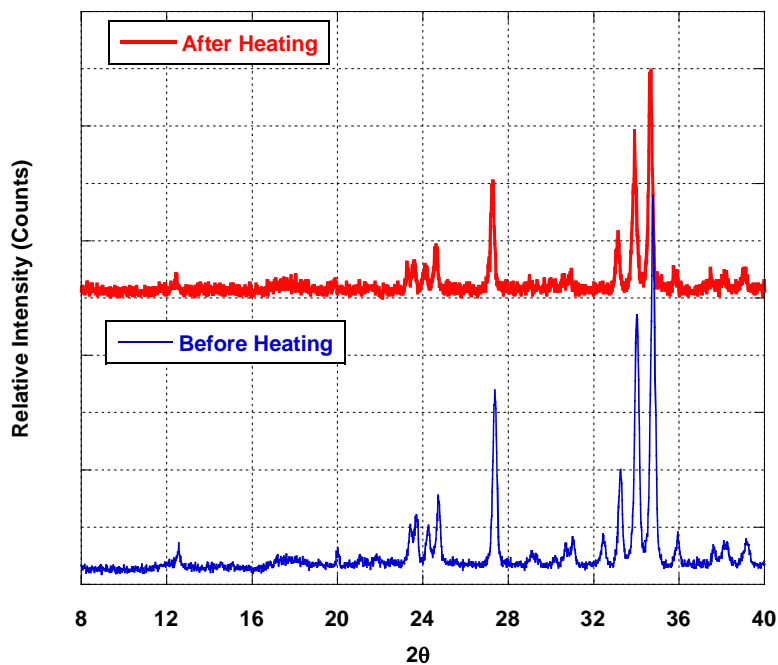


Figure 4.4.10 XRD analysis of sodium sulfate dicarbonate obtained from evaporation of an aqueous solution of Na_2CO_3 and Na_2SO_4 (mole ratio 6:1) with EDTA before and after exposure to 200 °C.

A sample of the sodium sulfate dicarbonate was exposed to 200 °C for an hour. As shown in Figure 4.4.10, an XRD analysis revealed no changes in the crystal after exposure to the elevated temperature. The PLM observation in Figure 4.4.11 also showed no significant changes in the optical properties of the sample. Exposure to heat did not affect the optical properties of the crystals suggesting that there are no hydrates and these hexagonal structures are stable.

These results confirm that sodium sulfate dicarbonate is a stable phase and does not readily transform into other Na_2CO_3 - Na_2SO_4 salts at industrial process conditions.

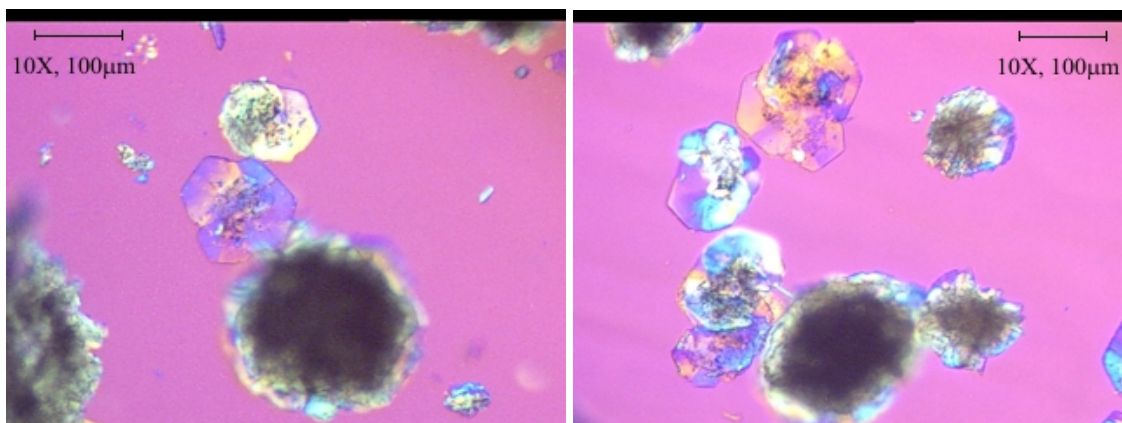


Figure 4.4.11 Photomicrographs of sodium sulfate dicarbonate crystals before (left) and after (right) heating to 200°C.

It can also be concluded from these results that only one crystal phase of sodium sulfate dicarbonate with two apparent habits can result from evaporative crystallization of aqueous solutions of Na_2CO_3 and Na_2SO_4 in the mole ratio 6:1.

4.5 Stability of Crystal Samples on Storage

The sodium sulfate dicarbonate crystal samples produced during this work were kept in a desiccator to avoid contact with moisture and air as prior work by Shi and Euhus suggested there is a possibility of sample degradation after exposure to moist ambient air and/or CO_2 . Gradual increase of weight measured on oven dried (200°C) crystals of sodium sulfate dicarbonate, burkeite, thermonatrite and anhydrous sodium carbonate that is left in ambient air confirmed that they are highly hygroscopic. According to Datta (2002) the normal conditions of the atmosphere encourage the formation of trona ($\text{Na}_2\text{CO}_3 \cdot \text{NaHCO}_3 \cdot 2\text{H}_2\text{O}$) in wet salt mixtures containing thermonatrite. Johnson et al. (2003) also mentioned the possible effect of dissolved carbon dioxide on the stability of precipitated phases of different inorganic salts.

Figure 4.5.1 is the photomicrograph of a sample that had been exposed to ambient air for about a week. Based on similar observations by Datta (2002), it is thought that the thin monoclinic rod-like crystal is trona. The crystal is noticeably larger than rod crystals that formed sodium sulfate dicarbonate. We speculate based on early work (see Figure 4.1.1) that moisture from the air partially dissolved sodium sulfate dicarbonate which recrystallized at room temperature as a mixture of burkeite and thermonatrite, and further exposure to atmospheric CO_2 produced trona from thermonatrite component of the mixture.

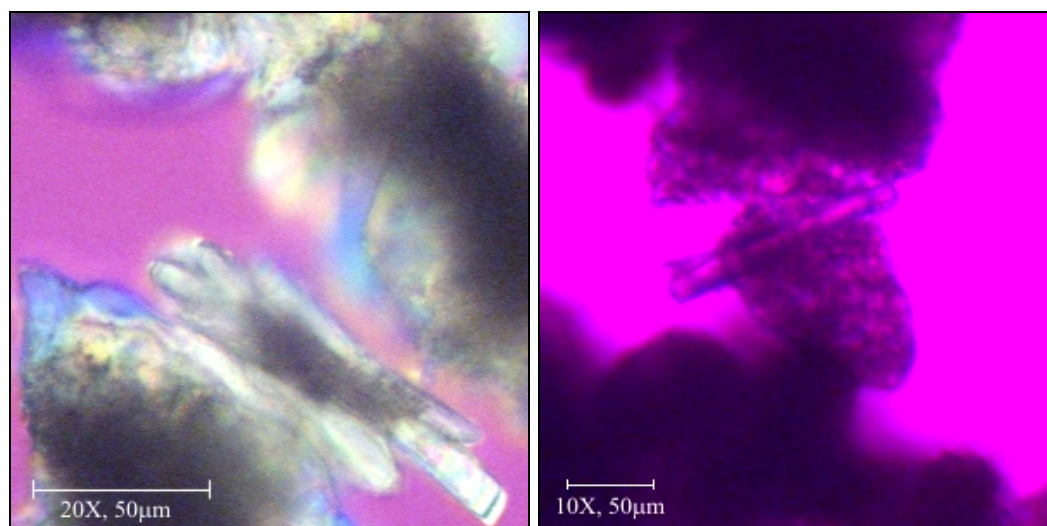


Figure 4.5.1 Photomicrograph showing possible trona formation in between sodium sulfate dicarbonate crystals due to prolonged exposure to ambient air.

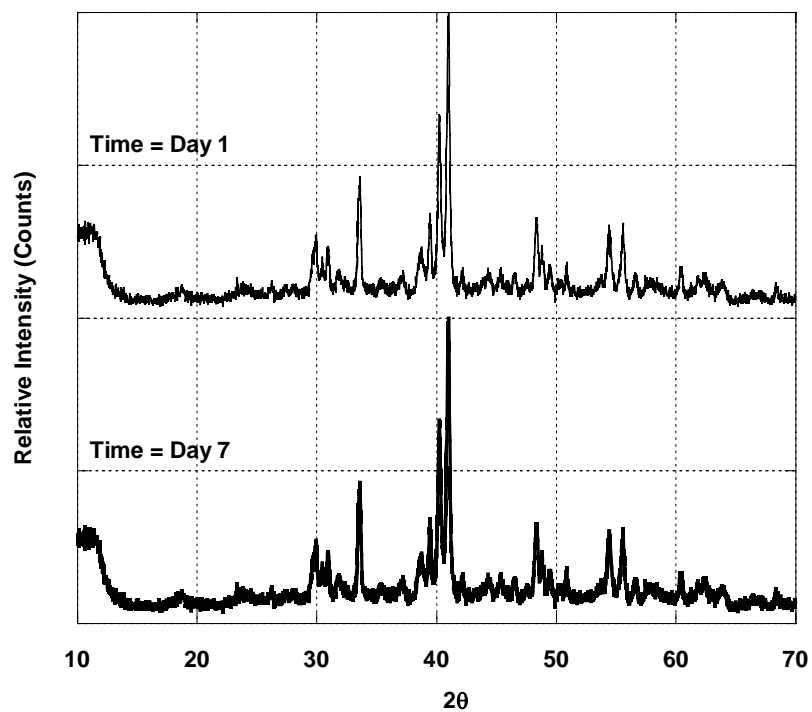


Figure 4.5.2 XRD results on sodium sulfate dicarbonate crystals stored for extended period of time in ambient air.

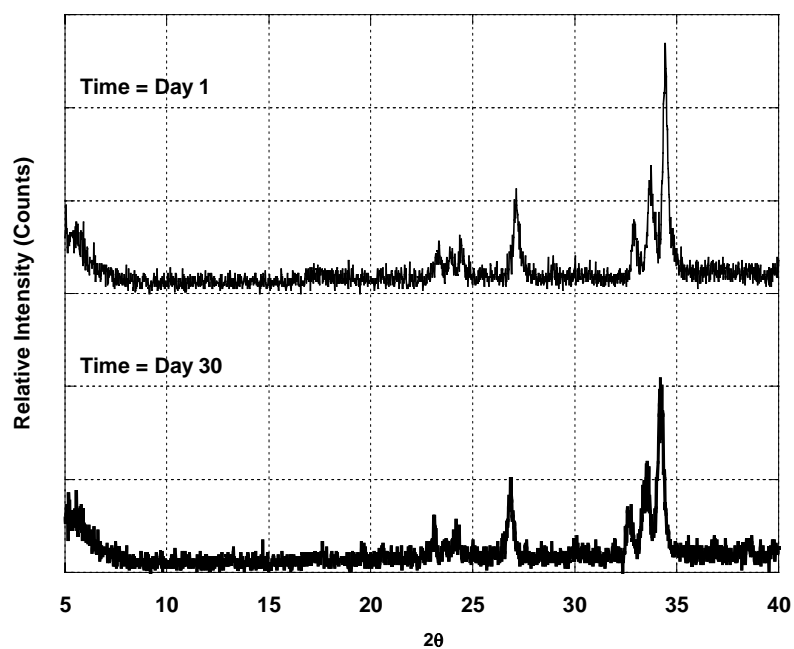


Figure 4.5.3 XRD results on sodium sulfate dicarbonate crystals stored for extended period of time under vacuum.

In one week period of time stored in ambient air of 50% relative humidity, there were no significant changes in the X-ray diffraction pattern for this sample which suggest trona formation was only trace amounts (see Figure 4.5.2). There was no apparent change for crystal samples that have been stored for a month or longer under vacuum (see Figure 4.5.3). The x-ray diffractogram stays exactly the same.

CHAPTER 5

CONCLUSIONS AND RECOMMENDATIONS

5.1 Conclusions

The experiments conducted in this work verify earlier findings that sodium sulfate dicarbonate is a unique phase that can be crystallized from aqueous solutions of Na_2CO_3 and Na_2SO_4 . Sodium sulfate dicarbonate is the predominant species crystallized from the evaporation of 6:1 molar ratio aqueous solution of Na_2CO_3 and Na_2SO_4 at 115 °C.

Agglomerates of rod-like crystals were the dominant form of sodium sulfate dicarbonate observed in this work. Agglomerate formation is influenced by reactant concentration and mixing intensity. If no EDTA is added to sequester trace amounts of calcium ions, a stable, hexagonal shape of sodium sulfate dicarbonate crystals can form. The hexagonal shape sodium sulfate dicarbonate crystals appear to grow under lower supersaturation condition. Lower supersaturation at nucleation reduced the formation of rod-like crystals, which have stronger tendency to agglomerate compared to the hexagonal habit.

Both crystal habits of sodium sulfate dicarbonate appear to be chemically stable at 115°C. This unique double salt does not transform or degenerate to other species when kept in contact with its mother liquor for prolonged times or when exposed to air at a temperature of 200 °C. It can be concluded that sodium sulfate dicarbonate is not a metastable or transient species.

Sodium sulfate dicarbonate isolated from its mother liquor will form trona on contact with water vapor and carbon dioxide in ambient air. Therefore, crystals obtained

from this system must be protected from air contact to avoid trona formation between sampling and analysis.

This work advanced several experimental methods in this research area. The method of isolating crystals was improved to minimize the risk of contaminant crystallization inside the filter. Crystal identification by polarized light microscopy and phase identification by XRD provided new data that are useful for analysis and comparison in future work.

5.2 Recommendations

5.2.1 Molecular level stability investigation

The basic crystal structure of sodium sulfate dicarbonate has not yet been reported, and my work was limited in the ability to produce large single crystals of burkeite and sodium sulfate dicarbonate for structural characterization using single crystal X-ray diffraction. This data is needed to develop a detailed structural model of sodium sulfate dicarbonate, which can then be used to explain its stability on molecular level by, e.g., Rietveld analysis to examine distortions or dislocations in the crystal structure during heating, aging, and other environmental changes.

An interesting area to explore is generation of larger single crystals of burkeite and sodium sulfate dicarbonate at 115°C by varying levels of calcium ions which may affect the size of single crystals attained before agglomeration. Note that the level of supersaturation may need to be carefully controlled in these experiments in order to induce growth and minimize agglomeration of smaller particles. The mixer rotation speed can be set for just enough turbulence to suspend the particles and avoid excessive

agitation that might contribute to crystal breakage and agglomeration. This will require improved Reynolds number calculation based on size and shape of the mixer blades.

5.2.2. Properties of different sodium sulfate dicarbonate crystal habits

The discovery of different crystal habits of sodium sulfate dicarbonate can be an important key to resolving the problems related to scaling in industrial spent pulping liquor concentrators. An evaluation of both adhesive and cohesive interactions between the two crystal shapes and heat transfer surfaces can be an interesting field of investigation. A test cell with well characterized heat transfer surface can be used in conjunction with controlled formation of the two crystals habits to observe impacts on fouling by specific crystals shapes.

APPENDIX A: POLARIZED LIGHT MICROGRAPHS OF SODIUM SALTS

Below are various polarized micrograph of sodium salts including hexagonal sodium sulfate dicarbonate crystals in mixtures with agglomerated rod-like crystals of the same species.

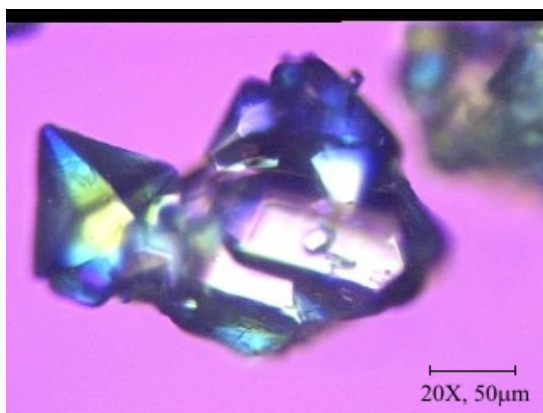


Figure A.1 Anhydrous Sodium Sulfate

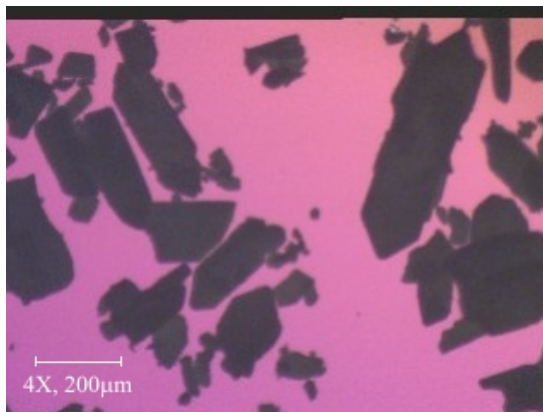


Figure A.2 Anhydrous Sodium Carbonate

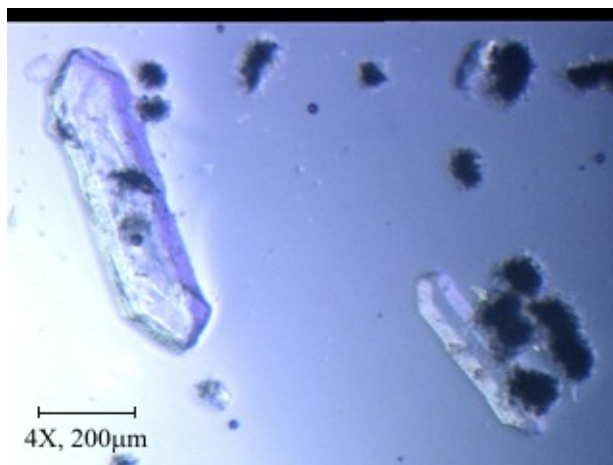


Figure A.3 Sodium Carbonate Monohydrate (transparent crystals) with Sodium Sulfate Dicarbonate Agglomerates (dark agglomerates)

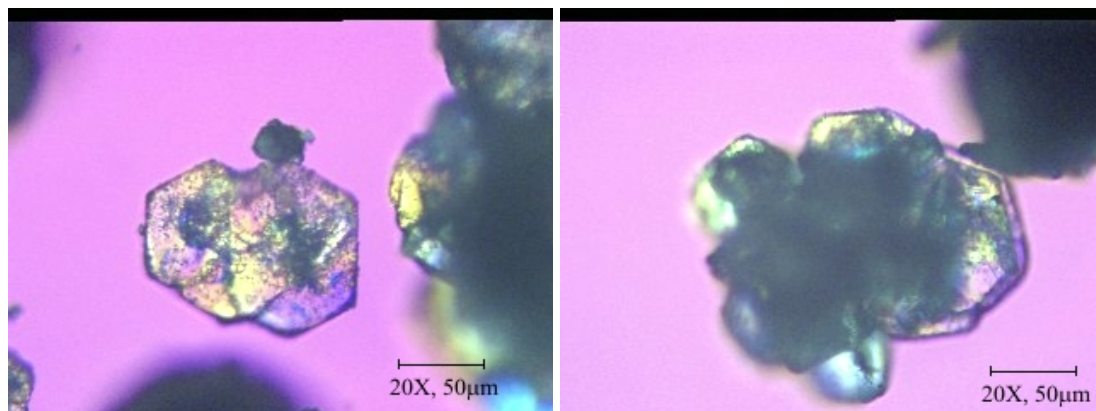


Figure A.4 Hexagonal Sodium Sulfate Dicarbonate aged for 12 hours without immersion medium shows hexagonal structure agglomerated like a flower petal.

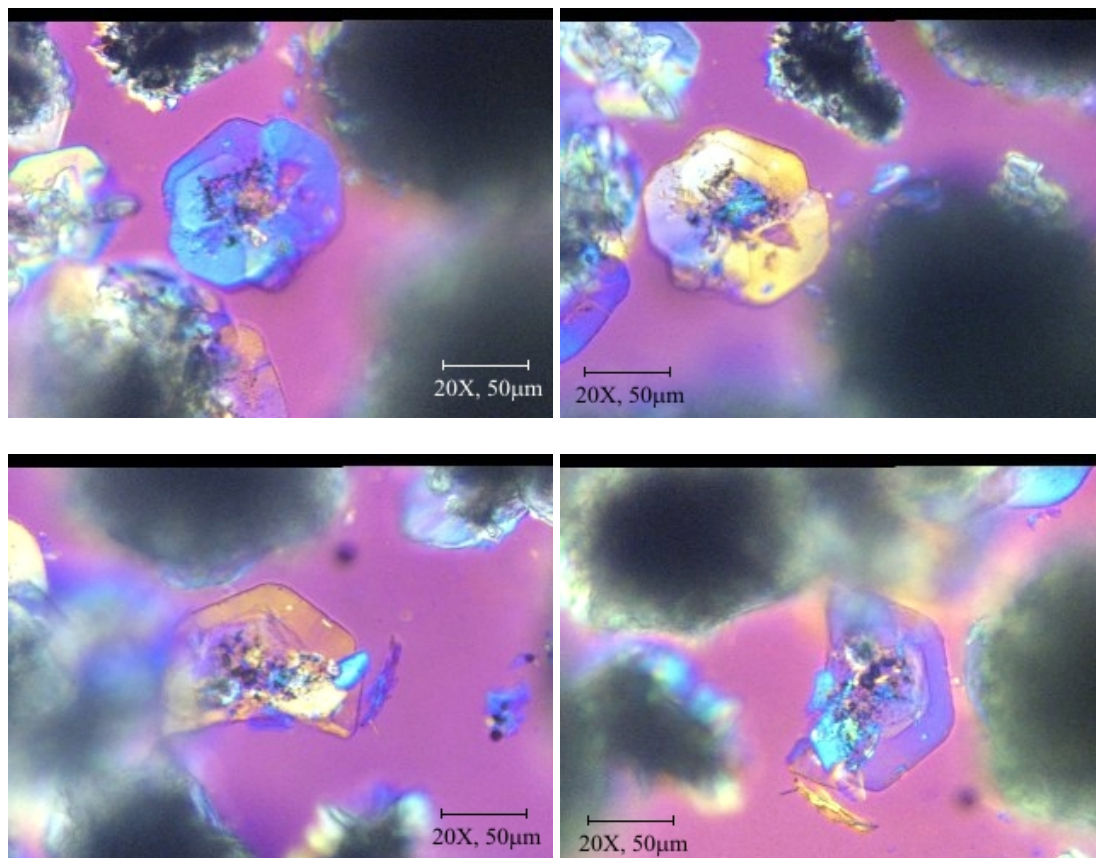


Figure A.5 Sodium Sulfate Dicarbonate aged for 12 hours immersed in Ethylene Glycol shows optical birefringence at different rotation angles.

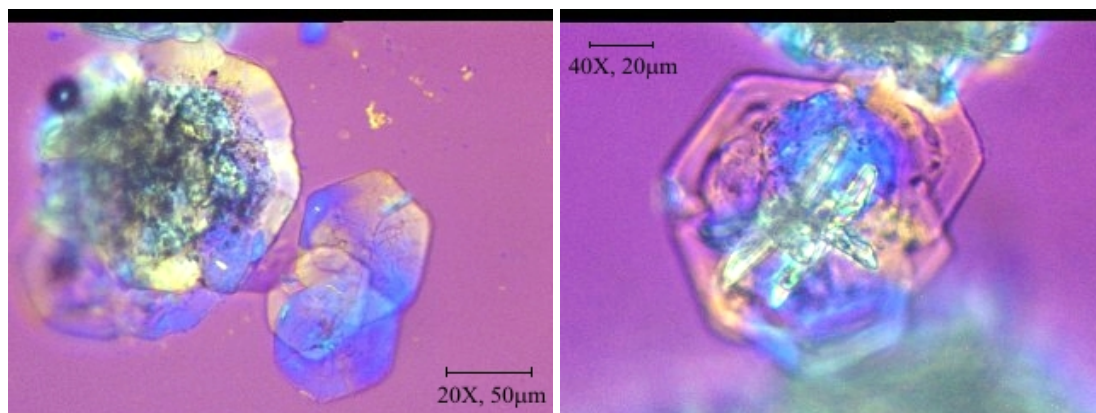


Figure A.6 Sodium Sulfate Dicarbonate aged for 12 hours (left) and 18 hours (right) immersed in Ethylene Glycol shows the hexagonal structure can grow from agglomerated core or a single rod crystal.

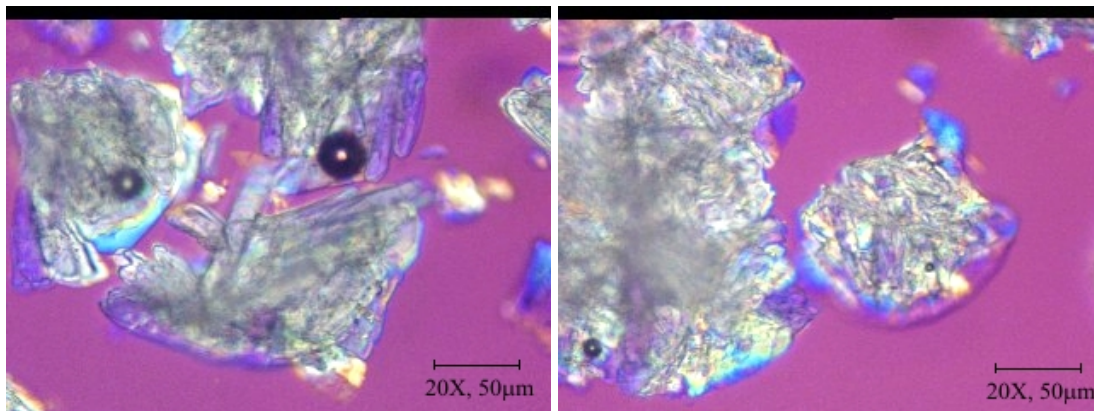


Figure A.7 Agglomerated rod-like crystals identified as Sodium Sulfate Dicarboxylate (aged for 18 hours) immersed in Ethylene Glycol

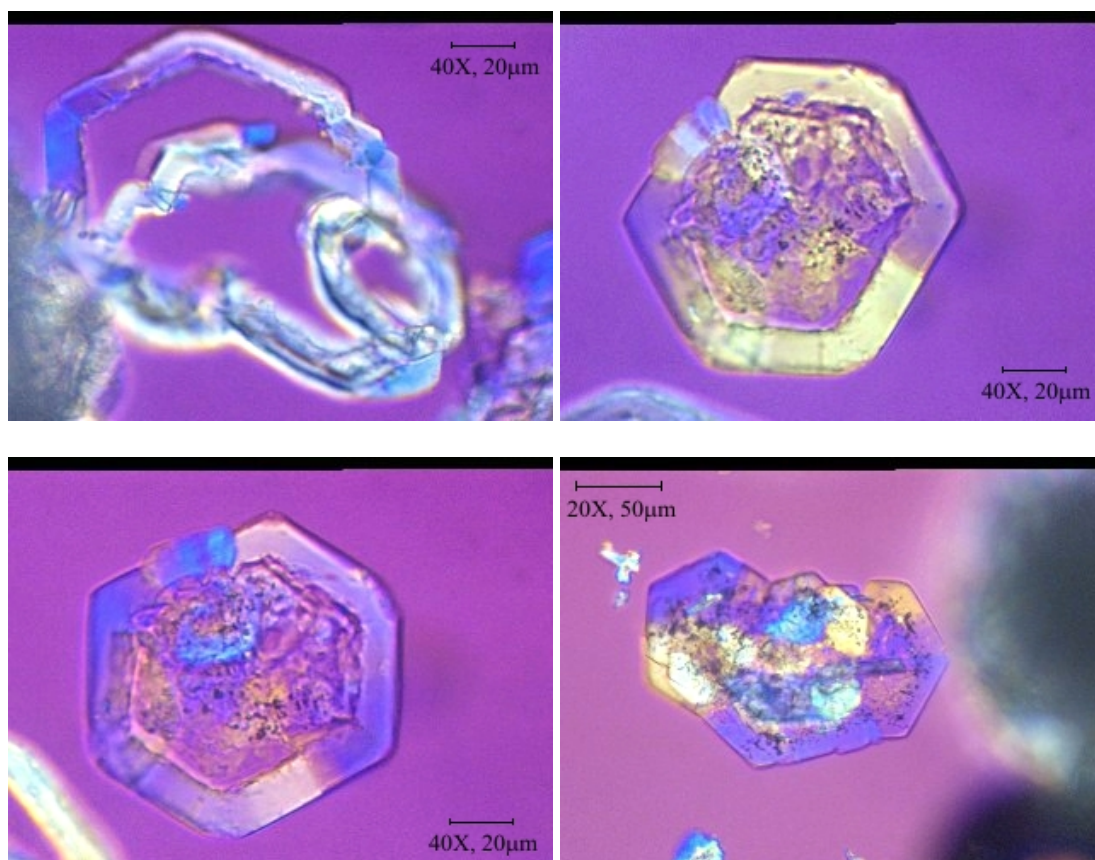


Figure A.8 Hexagonal Sodium Sulfate Dicarboxylate (aged for 18 hours) growing outward from a core single or agglomerated rod-like crystal.

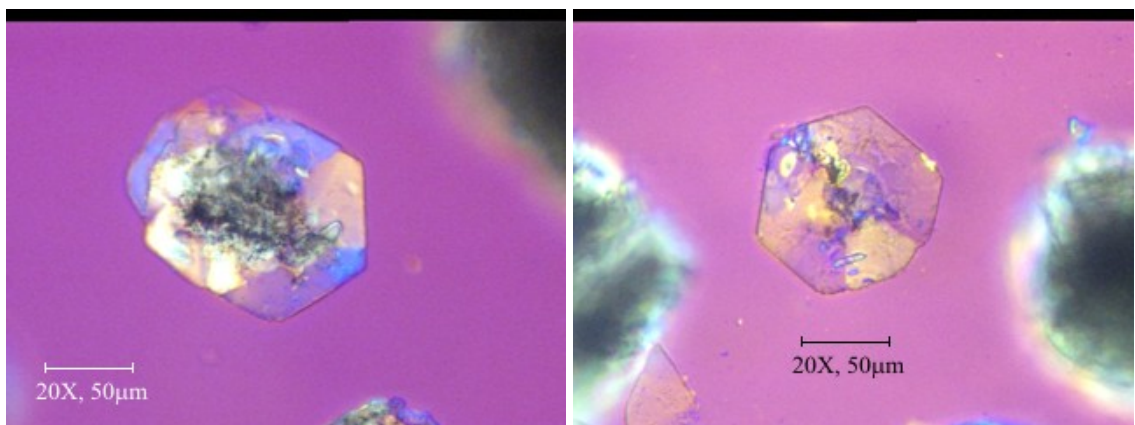


Figure A.9 Hexagonal Sodium Sulfate Dicarcarbonate (aged for 12 hours) showing colorful light refraction indicates crystal plane of {3, 1, 4}.

APPENDIX B: POWDER X-RAY DIFFRACTIONS OF SODIUM SALTS

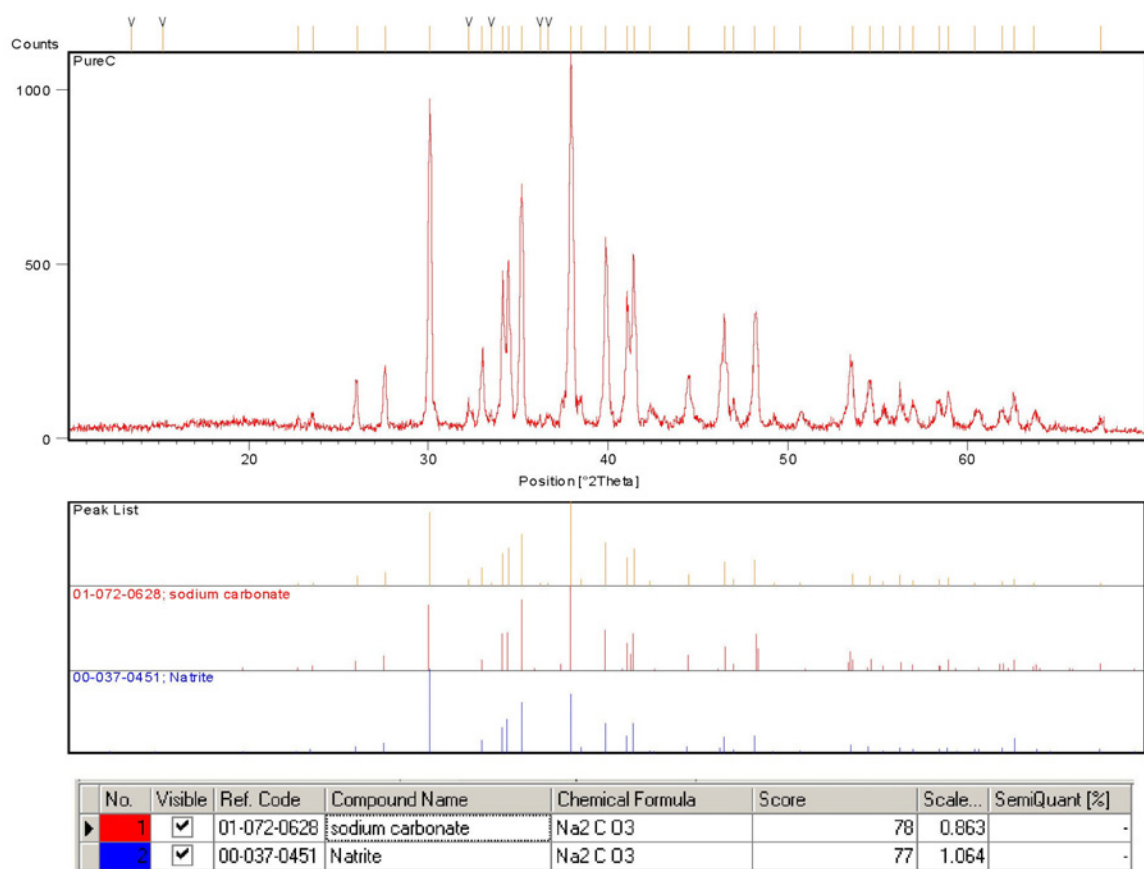


Figure B.1 Powder X-ray Diffraction of reagent anhydrous Sodium Carbonate crystals used in this work

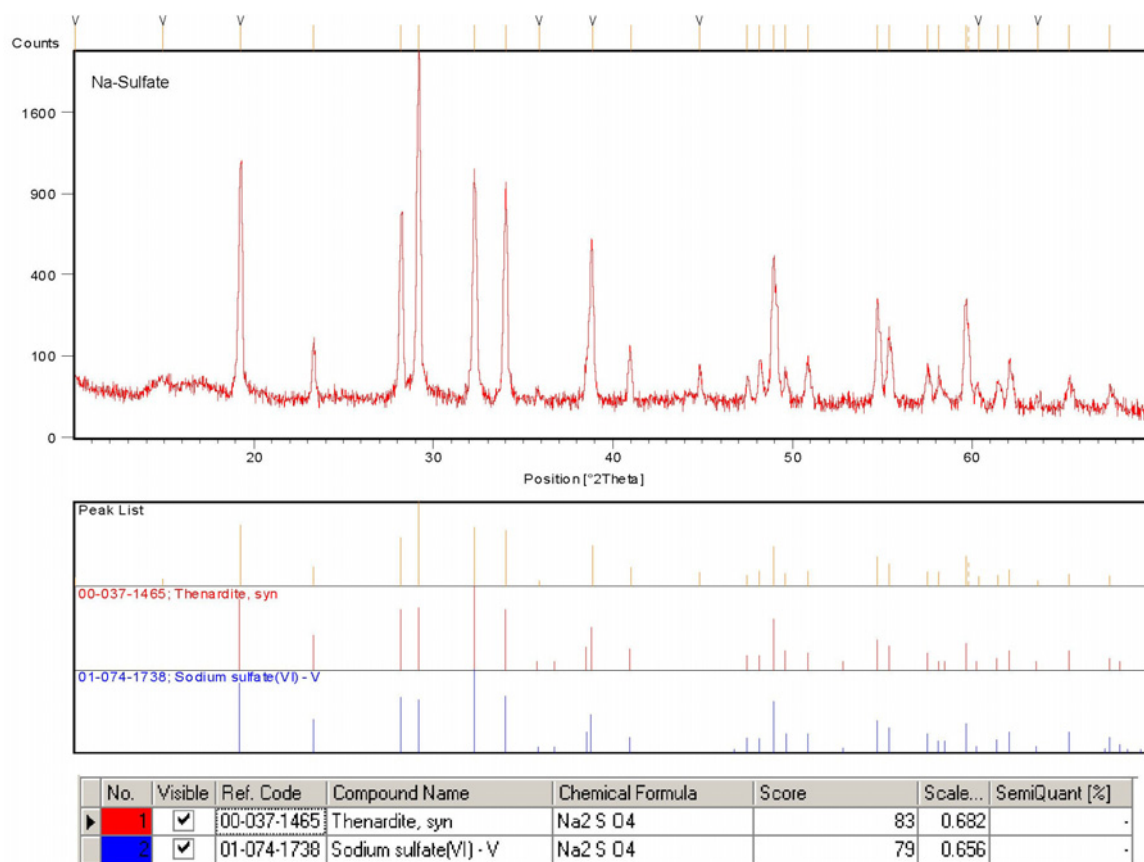


Figure B.2 Powder X-ray Diffraction of anhydrous Sodium Sulfate crystals used in this work

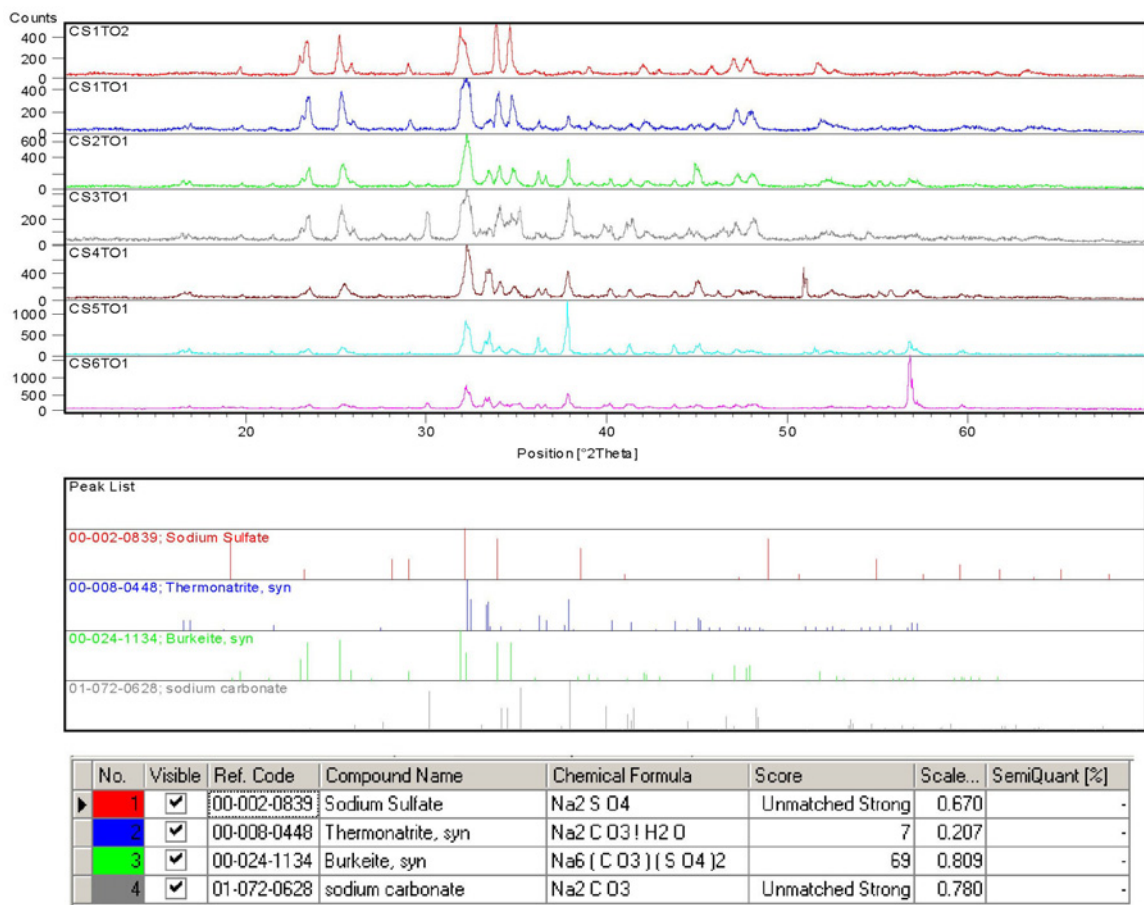


Figure B.3 Powder X-ray Diffraction of crystals from evaporation of the solution containing various molar ratio of Na₂CO₃ to Na₂SO₄ at 100°C.

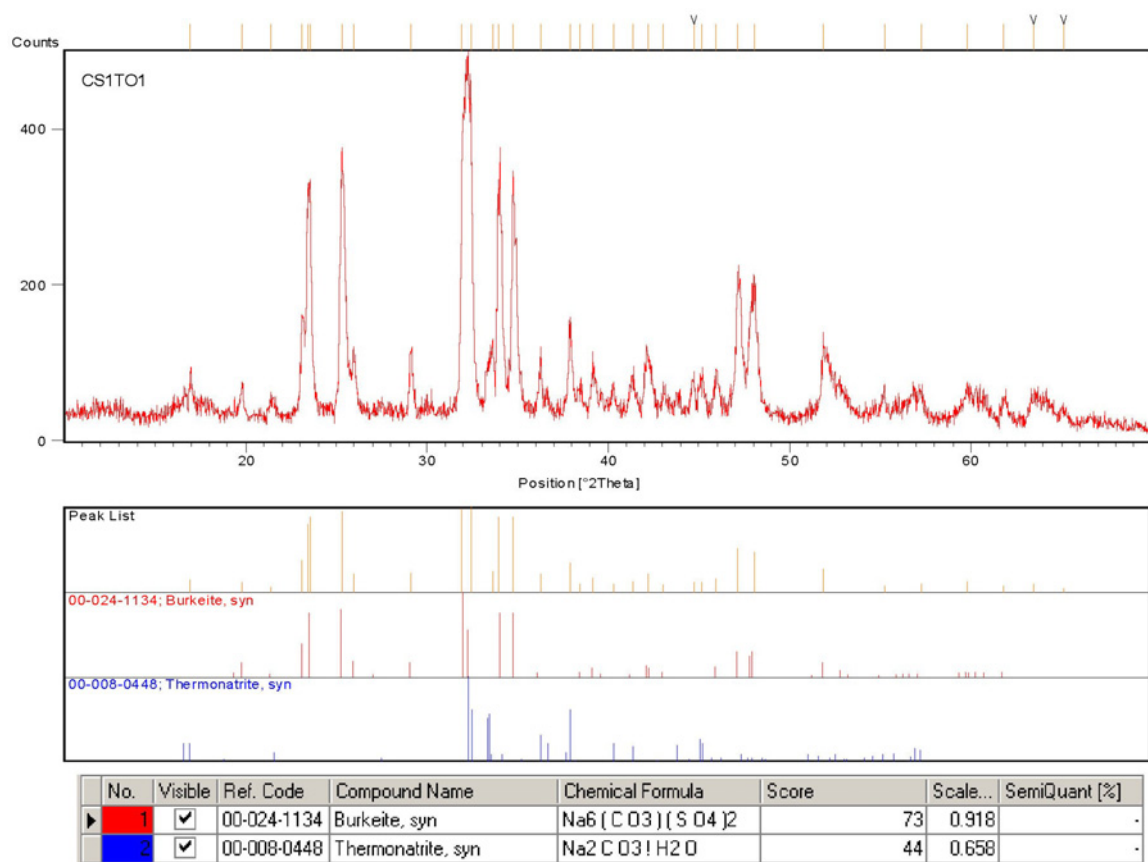


Figure B.4 Powder X-ray Diffraction of crystals from evaporation of aqueous solution of Na₂CO₃ to Na₂SO₄ at 1:1 mole ratio (100°C) shows a mixture of burkeite and thermonatrite.

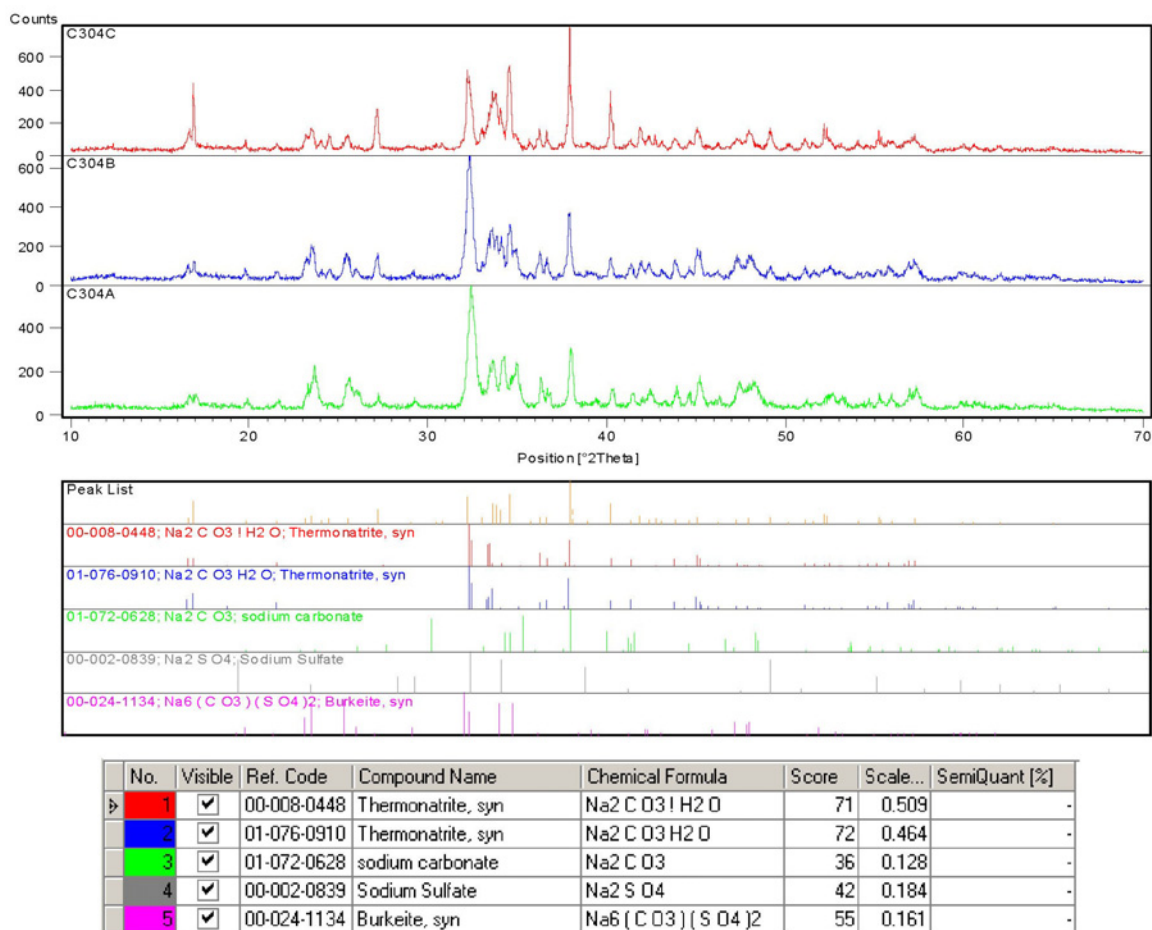


Figure B.5 Powder X-ray Diffraction of a mixture of sodium sulfate dicarbonate and thermonatrite crystals obtained from evaporation of an aqueous solution of Na₂CO₃ and Na₂SO₄ (6:1 mole ratio, without EDTA) after aging samples 0 (304A), 3 (304B) and 6 (304C) hours rinsed with ethanol.

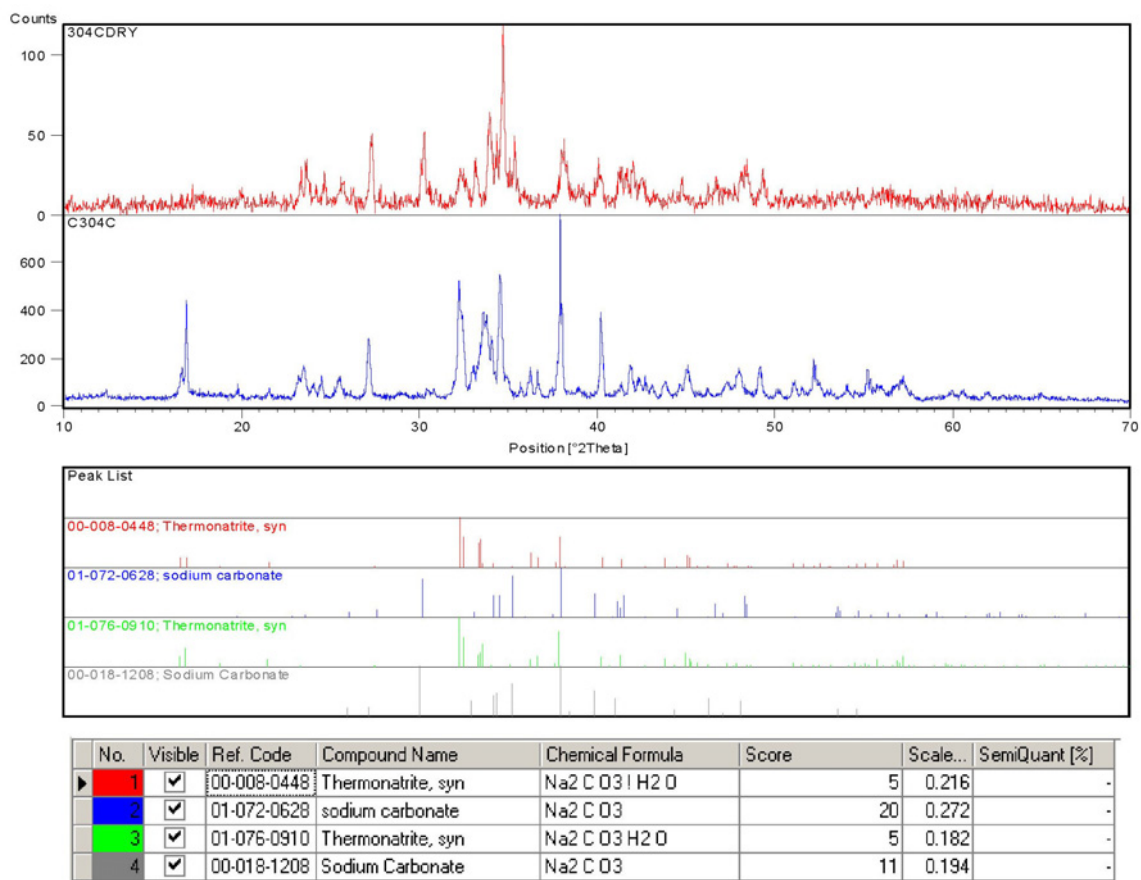


Figure B.6 Powder X-ray Diffraction of crystal mixture of sodium sulfate dicarbonate and thermonatrite harvested after 6 hours aging before and after exposure to 200°C.

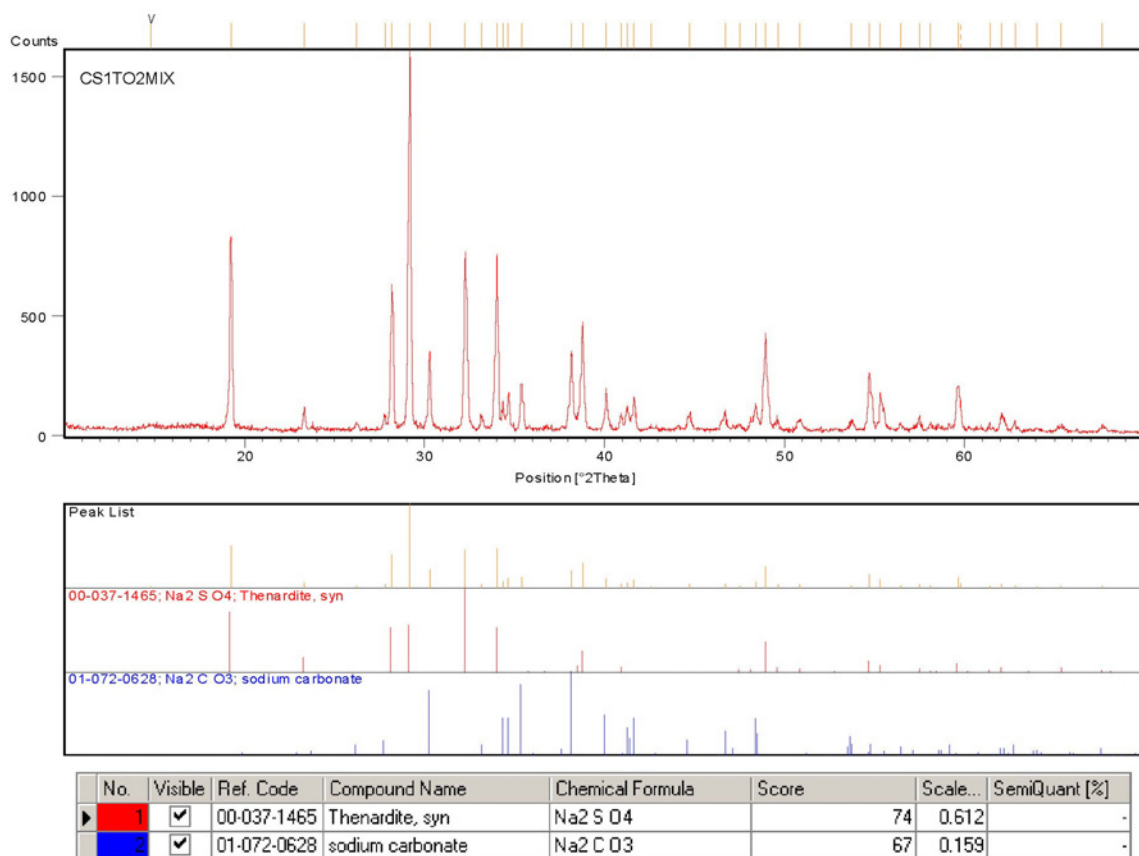


Figure B.7 Powder X-ray Diffraction of a mixture from anhydrous Na₂CO₃ and anhydrous Na₂SO₄ at 1:2 mole ratio shows integration of peaks from individual characteristic patterns.

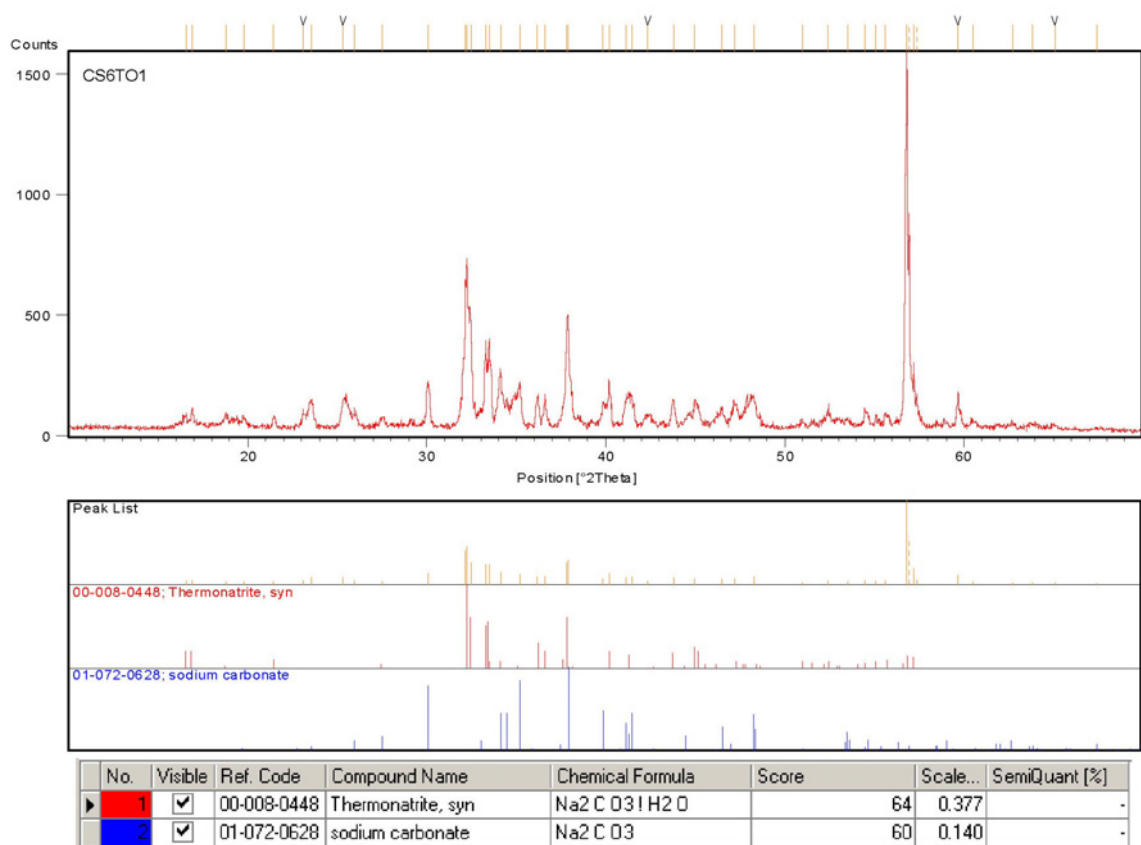


Figure B.8 Powder X-ray Diffraction of crystals from evaporation of an aqueous solution of Na₂CO₃ and Na₂SO₄ at 6:1 mole ratio (100°C) shows large thermonatrite content.

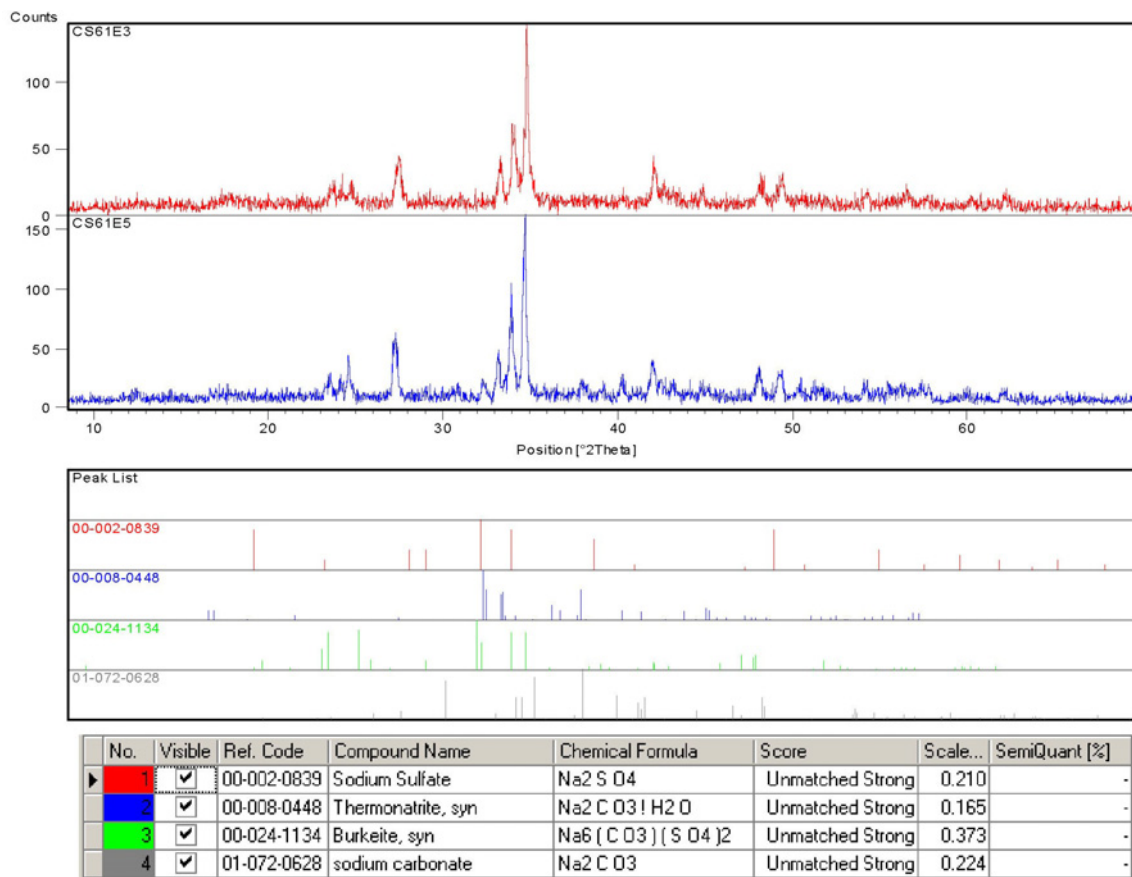


Figure B.9 Powder X-ray Diffraction of sodium sulfate dicarbonate crystals from evaporation of an aqueous solution of Na₂CO₃ and Na₂SO₄ at 6:1 mole ratio (115°C) with EDTA; sampled after aging 0 (CS61E3) and 24 hours (CS61E5).

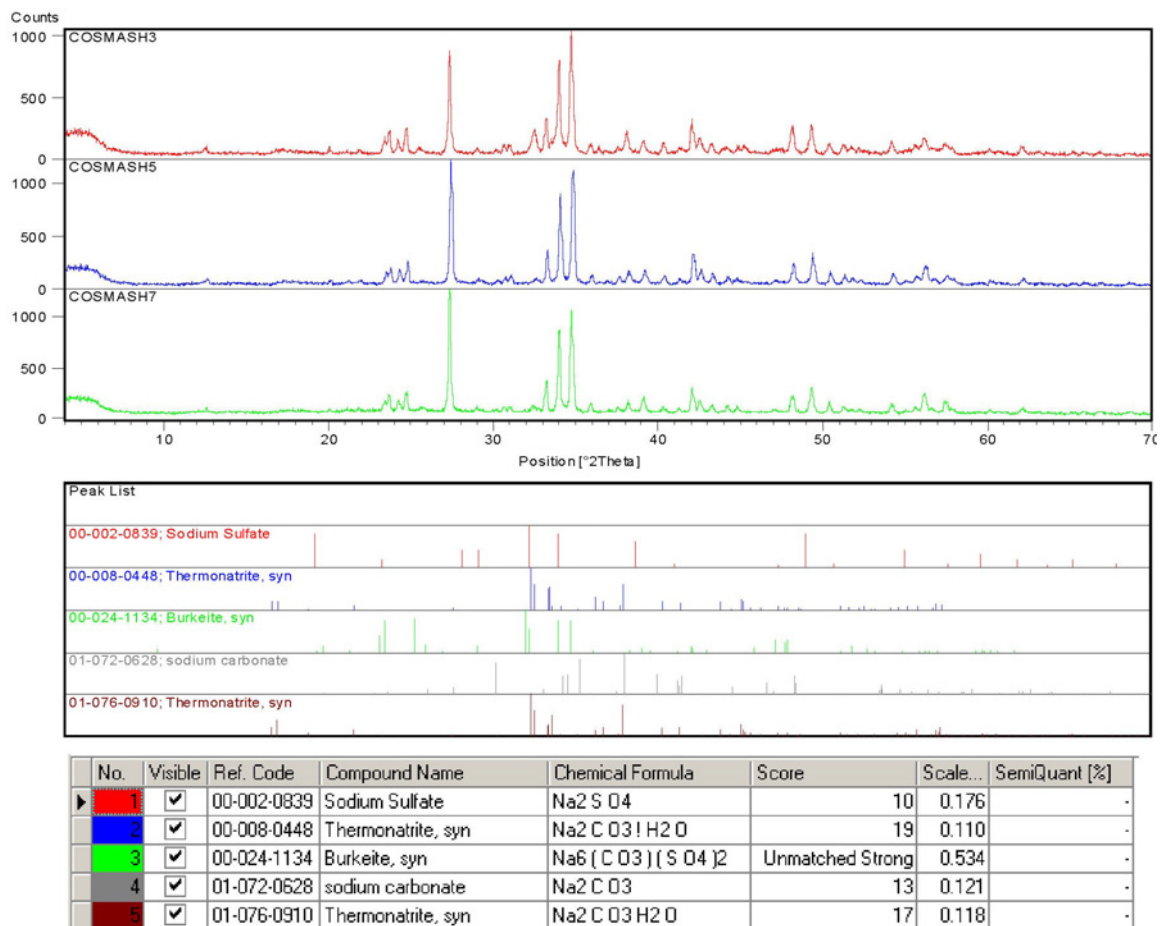


Figure B.10 Powder X-ray Diffraction of sodium sulfate dicarbonate crystals from evaporation of an aqueous solution of Na_2CO_3 and Na_2SO_4 at 6:1 mole ratio (115°C) without EDTA; sampled after aging 12 (COSMASH3), 18 (COSMASH5) and 34 hours (COSMASH7).

REFERENCES

1. Balarew, C., Calculation of the free Gibbs energy of phase transitions using solubility data. 1. The system $\text{Na}_2\text{SO}_4\text{--Na}_2\text{SeO}_4\text{--H}_2\text{O}$ at 15 °C: Stable and metastable equilibria*, *Pure Appl. Chem.*, Vol. 74, No. 10, pp. 1793–1800, 2002.
2. Caspari, W. A., “The System Sodium Carbonate-Sodium Sulphate-Water,” *Journal of the Chemical Society*, 125: 2381-2387 (1924)
3. Chung, F.H., Quantitative interpretation of X-ray diffraction patterns of mixtures. III. Simultaneous determination of a set of reference intensities *J. Appl. Cryst.* (1975). 8, 17-19.
4. Datta S., Thibault Y., Fyfe W.S., Powell M. A., Hart B.R., Martin R. R., and Tripathy S., Occurrence of trona in alkaline soils of the Indo-Gangetic Plains of Uttar Pradesh (U.P.), India, *Episodes*, December 2002, Vol. 25, no. 4, 236-239.
5. Euhus, D.D., Nucleation in Bulk Solutions and Crystal Growth on Heat-Transfer Surfaces during Evaporative Crystallization of Salts Composed of Na_2CO_3 and Na_2SO_4 , Ph.D. Thesis, Georgia Institute of Technology, 2003
6. Forbes, R.T.; York, P.; Fawcett, V.; Shields L., Physicochemical properties of salts of p-aminosalicylic acid. I. Correlation of crystal structure and hydrate stability. *Pharmaceutical Research*, 1992, Vol. 9, No. 11.
7. Frederick, W.J. and DeMartini, N., Aqueous System Solubility Results, Institute of Paper Science and Technology, Internal Report, Atlanta, GA (1999)
8. Frederick, W.J., Shi, B., Euhus, D.D., Rousseau, R.W., Crystallization and control of sodium salt scales in black liquor concentrators, *TAPPI Journal*, June 2004, Vol. 3(6).
9. Giulietti, M.; Seckler, M. M.; Derenzo, S.; M.I.R; Cekinski, E., Industrial Crystallization and Precipitation from Solutions: State of the Technique. *Brazilian Journal of Chemical Engineering* 2001, 18, (4).
10. Giuseppetti, G., Mazzi, F. and Tadini, C., “The Crystal Structure of Synthetic Burkeite: $\text{Na}_2\text{SO}_4(\text{CO}_3)_t(\text{SO}_4)_{1-t}$,” *Neues Jahrbuch fur Minerologie, Monatshefte*, 5: 203-221 (1988)
11. Green, S. and Frattali, F., “The System Sodium Carbonate-Sodium Sulfate-Sodium Hydroxide-Water at 100°C,” *Journal of American Chemistry Society*, 68: 1789-1794 (1946)

12. Green, S.; Frattali, F., The system sodium carbonate – sodium sulfate – sodium hydroxide - water at 100°C., J. Am. Chem. Soc. 1964. (68). p. 1789-1794.
13. Harris, M.J.; Dove, M.T.; Godfrey, K.W., A single-crystal neutron scattering study of lattice melting in ferroelastic. J. Phys.: Condens. Matter, 1996, Vol. 8, 7073-7084.
14. Hatakka, H.; Alatalo, H.; Palosaari, S., Effect of Impurities and additives on Crystal Growth, CST Workshop in Separation Technology at Lappeenranta, August 16-19, 1998
15. Hatakka, H.; Oinas, P.; Reunanen, J.; Palosaari, S., The Effect of supersaturation on agglomeration, Symposium on Crystallization and Precipitation at Lappeenranta, May 1997.
16. Helvenston, E. P.; Stewart, D. A.; Christi, C. Double Salt Having the Formula $(\text{Na}_2\text{SO}_4)_4(\text{Na}_2\text{CO}_3)_9$. U.S. Patent 3,493,326, 1970.
17. Johnson, C.D.; Skakle, J.M.S.; Johnston, M.G.; Feldman, J.; Macphee, D.E., Hydrothermal synthesis, crystal structure and aqueous stability of two cadmium arsenate phases, $\text{CdNH}_4(\text{HAsO}_4)\text{OH}$ and $\text{Cd}_5\text{H}_2(\text{AsO}_4)_4 \cdot 4\text{H}_2\text{O}$, J. Mater. Chem., 2003, 13, 1429-1432.
18. Khlapova1, A.N.; Kovaleva, E.S, The hexagonal burkeite solid solution (-phase) in the Na_2SO_4 – Na_2CO_3 system, Journal of Structural Chemistry, 4(4): 517 – 523, 1963.
19. Kim, Y.-s.; Paskow, H.C.; Rousseau, R. W.; Propagation of Solid-State Transformations by Dehydration and Stabilization of Pseudopolymorphic Crystals of Sodium Naproxen, Crystal Growth & Design, 5 (4), 1623 -1632, 2005.
20. Larson, M.A. and Garside, J., Solute Clustering in Supersaturated Solutions, Chemical Engineering Science, 41: 1285-1289 (1986)
21. Maksimov, I.L.; Sanada, M.; Nishioka, K. Energy barrier effect on transient nucleation kinetics: Nucleation flux and lag-time calculation, Journal of Chemical Physics 113 (8), 2000
22. Mersmann, A. (ed.), Crystallization Technology Handbook: 24, Marcel Dekker, New York (1995)
23. Mullin, J.W., Crystallization, 4th ed., Butterworth-Heinemann, Oxford (2001)
24. Novak, L. Sodium Salt Scaling in Connection with Evaporation of Black Liquors and Pure Model Solutions. Ph.D. Thesis, Chalmers University of Technology, 1979

25. Oosterhof, H.; Witkamp, GJ.; Rosmalen, G.M.v., Antisolvent crystallization of anhydrous sodium carbonate at atmospheric conditions, *AIChE Journal*, Volume 47, Issue 3, 2001. Pages 602-608
26. Oosterhof, H.; Graauw, J.; Witkamp, GJ.; Rosmalen, G.M.v., Continuous Double Recrystallization of Light Soda Ash into Super Dense Soda Ash. *Crystal Growth & Design*, 2002, 2 (2), 151 -157.
27. Oosterhof, H.; Witkamp, GJ.; Rosmalen, G.M.v., Evaporative crystallization of anhydrous sodium carbonate at atmospheric conditions, *AIChE Journal*, Volume 47, Issue 10, 2001. Pages 2220-2225
28. Ryoo, R.; Jun, S., Improvement of hydrothermal stability of MCM-41 using salt effects during the crystallization process. *J. Phys. Chem B* 1997, 101, 317-310.
29. Schroeder, A., Berk, A., and Gabriel, A., Solubility Equilibria of Sodium Sulfate at Temperatures from 150 to 350°. II. Effect of Sodium Hydroxide and Sodium Carbonate, *Journal of the American Chemical Society*, 58: 843-849 (1936)
30. Seidell, A.; Linke, W., Solubility of inorganic and metal organic compounds. Vol. II., 4th ed., Van Nostrand, Princeton, 1965, p. 915, 938-939, 1122.
31. Shi, B., Crystallization of Solutes that Lead to Scale Formation in Black Liquor Evaporation, Ph.D. Thesis, Georgia Institute of Technology, 2002
32. Shi, B., Rousseau, R.W., Frederick, W.J. Jr. Nucleation of Burkeite from Aqueous Solutions and Black Liquor. *Proc. 2001 TAPPI-CPPA Intl. Chem. Recovery Conf., PAPTAC, Montreal*, p. 177-18.
33. Shi, B.; Frederick, W. J.; Rousseau, R. W., Effects of Calcium and Other Ionic Impurities on the Primary Nucleation of Burkeite, *Ind. Eng. Chem. Res.*, 2003, 42, 2861.
34. Shi, B.; Frederick, W.J. Jr.; Rousseau, R. W., Nucleation, growth, and composition of crystals obtained from solutions of Na_2CO_3 and Na_2SO_4 . *Ind. Eng. Chem. Res.* 2003, 42, 6343-6347.
35. Shi, B.; Rousseau R.W., Crystal properties and nucleation kinetics from aqueous solutions of Na_2CO_3 and Na_2SO_4 . *Ind. Eng. Chem. Res.* 2001, 40, 1541-1547.
36. Shi, B.; Rousseau, R.W., Structure of burkeite and a new crystalline species obtained from solutions of sodium carbonate and sodium sulfate. *J. Phys. Chem. B* 2003, 107, 6932-6937.

37. Swainson, I.P.; Dove, M.T.; Harris, M.J., Neutron powder diffraction study of the ferroelastic phase transition and lattice melting in sodium carbonate, Na_2CO_3 J. Phys.: Condens. Matter, 1995, Vol. 7, 4395-4417.
38. Vener, R.E. and Thompson, A.R., Solubility and Density Isotherms for Sodium Sulfate-Ethylene Glycol-Water,” Industrial and Engineering Chemistry, 41(10): 2242-2247 (1949)
39. [Http://Wikipedia.org](http://Wikipedia.org), Crystal Structure, April 14th, 2006.